NATIONAL AERONAUTICS AND SPACE ADMINISTRATION

Technical Memorandum 33-534

Solid Propulsion Advanced Concepts

Y. Nakamura

J. I. Shafer

JET PROPULSION LABORATORY

CALIFORNIA INSTITUTE OF TECHNOLOGY

PASADENA, CALIFORNIA

May 1, 1972

PREFACE

The work described in this report was performed by the Propulsion Division of the Jet Propulsion Laboratory.

ACKNOWLEDGEMENT

CONTENTS

CONTENTS (contd)

CONTENTS (contd)

ABSTRACT

In this study, the feasibility and application of a solid propulsion powered spacecraft concept to implement high-energy missions independent of multiplanetary swingby opportunities are assessed and recommendations offered for future work. An upper-stage, solid propulsion launch vehicle augmentation system was selected as the baseline configuration in view of the established program goals of low cost and high reliability. During the study, a new high-mass-fraction solid motor staging design, the conesphere motor concept, was conceived, and its anticipated performance predictions further enhanced the candidacy of the solid propulsion baseline configuration. A class of missions of increasing scientific interest was identified and the attendant launch energy thresholds for alternate approaches determined. Spacecraft and propulsion system data that characterize mission performance capabilities were generated to serve as the basis for subsequent tradeoff studies. A cost-effectiveness model was used for the preliminary feasibility assessment to provide a meaningful comparative effectiveness measure of the various candidate designs. The results substantiated the feasibility of the powered spacecraft concept when used in conjunction with several intermediate-sized launch vehicles as well as the existence of energy margins by which to exploit the attainment of extended mission capabilities. Additionally, in growth option applications, the employment of advanced propulsion systems and alternate spacecraft approaches appear promising.

I. INTRODUCTION

With the advent of the Pioneer F and G and the Outer Planets Project flights, the exploration of the outer planets will have begun. An increasing scientific interest will also be developing in more detailed investigations within the solar system as well as exploration beyond its outer fringes. Hence, a need exists to evaluate advanced propulsion system concepts for implementing these missions and to identify advanced technology developments required to bring the attendant propulsion capability to fruition. The advancement of propulsion technology has historically proven to be a long-lead development item. In order to ensure the availability of a suitable propulsion system in a time frame coincident with projected mission needs, it is imperative that mission application studies be instituted at an early date.

To this end, a preliminary study was initiated by the Propulsion Division of the Jet Propulsion Laboratory to investigate the use of energetic chemical rocket systems as a means of effecting reduced trip times for high-energy missions independent of multiplanetary swingby opportunities. The specific objective of this study was to evaluate the potential of utilizing a solid rocket powered spacecraft concept to augment standard launch vehicle performance and achieve the development of early, low-cost solar escape probes. This class of mission was selected as being one which could test the utility of such a propulsion concept. An outgrowth of the study included a characterization of the required solid motor propulsive system as well as a delineation of the advantages and disadvantages of the most promising designs in comparison with alternate approaches.

Included in the study was an analysis of the requirements for the solid propulsion stages, propulsion technology, mission and spacecraft, and interface development. Although the study focused on the determination of solid propulsion stage and propulsion technology requirements, it was also

necessary to investigate related peripheral areas such as mission, spacecraft, and interface development in order to lend credence to the results derived.

Ground rules under which this study was conducted included the constraints of (1) ballistic trajectory, (2) Jupiter swingby as an alternate to direct flight, (3) use of standard launch vehicles, and (4) limitation of the science package to particle and field measurements only.

Based upon the results of past studies and intuitive engineering judgment, a solid propulsion approach was selected as the appropriate baseline configuration for evaluation in light of the established program goals of low cost and high reliability. It was not intended for the results of the study to demonstrate that a solid propulsion system was the only feasible method of implementing this design approach. Rather, it was anticipated that solid propellant rocket motors would provide a suitable representative propulsive system for evaluating the gross feasibility of the powered spacecraft concept accomplishing a given class of missions, and for identifying critical technologies that must be addressed during the advanced development phase.

In addition, as the study progressed and the payload and launch energy margins of competitive systems were characterized, a wider spectrum of sophisticated scientific missions that might also be candidates for this concept were identified for consideration in future studies.

II. SUMMARY

A class of missions of scientific interest was identified in which there is a need for a simple, energetic propulsion system. A representative scientific payload and spin-stabilized spacecraft necessary to implement these missions were determined and their weight and power characteristics established. Parametric data were developed to interrelate solar system escape capability as a function of payload, solid motor spacecraft escape propulsion performance, and basement launch vehicle characteristics. Program goals for mission flight times were also established in an attempt to capitalize on the spacecraft and electronics technologies that would be developed as a result of the Pioneer and Outer Planets Project flights.

Candidate launch vehicle assemblies were assessed as a function of their launch energy output in meeting established program goals. Performance characteristics of state-of-the-art and advanced technology solid propulsion capabilities were included in the assessment of competitive powered spacecraft configurations. A cost-effectiveness assessment model was used as the basis for the preliminary feasibility study. The performance characteristics of the more promising designs were compiled and their out-of-ecliptic performance capabilities determined. The advantages and disadvantages of this simple, low-cost mission were determined in comparison with alternate systems.

The study produced the following conclusions:

1. The gross feasibility of adapting solid propulsion to the powered spacecraft concept to accomplish solar escape and out-of-ecliptic missions in conjunction with existing and projected basement vehicles has been substantiated.

2. There are no apparent operational or technological limitations that would severely hamper the mechanization of this conceptual approach based upon a conservative estimate of technology advancements.

3. Launch energy margins exist for each of the selected propulsion system assemblies to accommodate nominal perturbations in ground rule constraints and to exploit evolutionary growth options.

4. Embodiment of advanced technologies and innovations such as the high-mass-fraction motor and advanced data management techniques should greatly enhance the spacecraft/mission capabilities.

III. APPROACH

The technical approach adopted during this study included implementation of the following tasks:

1. Establishment of representative payloads for direct solar system escape and for probes utilizing Jupiter swingby.

2. Determination of solid motor characteristics for both current and advanced technology configurations.

3. Selection of representative launch vehicles for analysis.

4. Development of parametric solar system escape and out-of-the-ecliptic capability for varying payload, solid motor characteristics, number of stages, and launch vehicles. Evaluation of the benefits of advanced solid motor designs for this application, advantages and disadvantages of Jupiter swingby, effect of staging, etc.

5. Formulation of solid motor size and technology requirements.

6. Determination of the advantages and disadvantages of this simple, low-cost mission in comparison with alternates.

A. Concept Description

The concept depicting launch vehicle augmentation with a simple energetic four-stage spacecraft escape propulsion system is illustrated in Fig. 1, employing a space shuttle as the basement launch vehicle. However, this conceptual approach could be implemented equally well through the use of several existing intermediate-size launch vehicles (i.e., Titan IIID (7)/Centaur family of vehicles). Furthermore, this approach would be equally applicable to any future missions, such as solar escape probes, out-of-ecliptic probes, and rendezvous encounters, in which energetic propulsion capability will be required to reduce mission flight time to reasonable values.

Potential benefits to be derived include early exploration of regions beyond the solar system which are of significant scientific interest. In addition, if the concept proves feasible, it could provide for solar escape missions without the need for development or utilization of expensive launch vehicles. Thus, the concept offers the advantages of achieving early, low-cost missions with reduced flight times and high reliability.

The effect of augmenting standard launch vehicles is illustrated in Fig. 2. A displacement-flight time histogram associated with solar escape threshold, corresponding to a vis-viva energy level (C_3) of ~152 km^2/s^2, is defined by the upper solid curve. As depicted in the figure, the use of standard launch vehicles as energetic as the Saturn V booster alone is still inadequate for placing a 272-kg (600-lb_m) payload into a solar escape mission. The C_3 output for a shuttle with a Centaur upper stage also falls short of realizing a solar escape mission for an identical spacecraft payload (i.e., C_3 = 144). In contrast, the addition of a four-stage solid spacecraft escape propulsion system to a standard Titan IIID/Centaur (STR)/BII (2300) launch vehicle provides a sufficient vis-viva energy level to yield solar escape missions for the representative payload selected and flight times of the order of 10.5 years out to distances as far as 40 AU. Shorter flight times of ~6.3 years are achievable to 40 AU with Jupiter swingby. Similarly, it can be shown that the substitution of a four-stage solid spacecraft escape propulsion system for the Centaur upper stage on the shuttle makes the launch vehicle assembly capable of implementing an equivalent solar escape mission.

As a major study program objective, C_3 goals of 152 and 250 km^2/s^2 were adopted for Jupiter swingbys and direct flights, respectively. At these launch energy levels, trip times on the order of 10 years or less can be anticipated to the outer fringes of the solar system. These trip times are comparable to, or better than, the flight times derived from multiplanetary swingby opportunities. In selecting flight times on this order, the mission/spacecraft would capitalize upon the spacecraft and electronics technologies that may have been developed as a result of future missions such as the Outer Planets Project.

B.   Methodology

The methodology adopted during the conduct of this study included the generation of parametric data interrelating mission flight time t_f, distance from the sun D, and vis-viva energy level C_3 (Fig. 3a). Once these launch energy thresholds were established, candidate launch vehicles were assessed in light of their C_3 output (Fig. 3b) as a function of number of stages n and characteristic propulsion payload mass (i.e., spacecraft mass) M_{PL}. The most promising launch vehicles underwent a further staging velocity optimization study (Fig. 3c) to determine the maximum C_3 output possible as a function of staging velocity and n. Influence coefficients were formulated

to identify critical parameters and to facilitate future tradeoff studies (Fig. 3d). An effectiveness measure criterion, mission worth, was also formulated as a function of mission profile (Fig. 3e). From the foregoing relationships, a plot that interrelates mission worth vs. time of flight and C_3 levels (Fig. 3f) for the various candidate launch vehicles was constructed. Corresponding relationships between cost, number of stages, and gross stage weight M_0 (Fig. 3g) and reliability, flight time, and number of stages (Fig. 3h) were also established and used to assess the cost-effectiveness rating of candidate designs (Fig. 3i).

IV. MISSION/SPACECRAFT REQUIREMENTS

A. Spacecraft Investigations

Spacecraft investigations are necessary to size the payload weight, which in turn sizes the multi-staged solid propulsion systems that are of primary interest in this study. Scientists and spacecraft engineers at JPL and Ames Research Center who are familiar with particles and fields experiments and spacecraft design were interviewed so that representative payloads for solar system escape probes could be defined. Additionally, space regions of primary interest to the scientific community were identified (Fig. 4). These regions include (1) the Lyman-alpha region (where evidence of hydrogen leakage into the solar system from the interstellar medium has been observed) and (2) the sun's apex about the galactic center. Specific phenomena of scientific interest are:

1. Ionization of neutral atoms, beginning at a distance of about 5 AU from the sun.

2. Cosmic-ray and magnetic field interactions, also beginning at 5 AU.

3. Solar wind shock formations, which could be located from 30 AU to larger distances.

There is scientific interest in these phenomena out to distances as far as 100 AU, which should, therefore, represent the maximum probe distance for purposes of this study.

A typical science package capable of carrying out the necessary experiments has been identified (Table 1), and consists of a helium vector magnetometer and plasma and cosmic-ray measurement devices. Corresponding component weights and power requirements estimated for the baseline science package are also given in Table 1.

Table 2 identifies the characteristics of a growth scientific package, whose addition in toto should enhance mission return by a factor of 2.

The weight of the attendant spacecraft necessary to implement these meaningful scientific experiments has been estimated (Table 3). It is anticipated that the spacecraft would be spin-stabilized and carry radioisotope thermoelectric generators (RTG) as the primary power source. In the

operational state, the generators would be deployed at the end of booms, well beyond the perimeter of the antenna reflector, to reduce the radiation environment within the equipment compartment and the magnetic influence of the RTGs on the magnetometer. An attitude control system consisting of monopropellant hydrazine thrusters would also be included to provide the necessary thrust vector alignment, communication pointing, guidance corrections, and despin maneuvers. The spacecraft would be equipped with a complete telemetry and data handling system, which would generate a data stream containing the output of scientific instruments and spacecraft equipment measurements. Major subsystems comprising the spacecraft are indicated in Table 3 along with their weight assignments. Gross spacecraft weights ranging from 258 to 408 kg (600 to 900 lb_m) have been predicted.

Although the scientists appear to prefer a spinning particles and fields science package, it is not mandatory that the spacecraft be spinning. A spinning spacecraft may be preferred, however, because of the resulting simplification to both spacecraft and solid stage design (i.e., elimination of gyro package, attendant logic, flight computers, etc.). The disadvantages of a spinning spacecraft include a degradation of the doppler cycle count and hence, spacecraft position determination. A spin-stabilized vehicle would further detract from the quality of active imaging devices that may be considered as a future evolutionary growth potential. Although there are several options available to the spacecraft designer to alleviate image smear, such as shortening exposure time, reducing vehicle spin rate, or providing some form of image motion compensation, the incorporation of these innovations is not without penalties.

B. Escape Propulsion Augmentation System

In order to establish the feasibility of this powered spacecraft concept, the following questions must be addressed:

1. Can the powered spacecraft concept be utilized in conjunction with standard basement vehicles to launch a low-cost particles and fields spacecraft out of the solar system?

2. What are the payload capability and mass?

3. What is the optimum number of stages and the best basement launch vehicle(s)?

4. Should conventional or advanced solid propulsion technology be used?

5. Should the payload be launched directly or with Jupiter swingby?

6. How does the staged solid propulsion concept compare with other methods of accomplishing the same mission?

7. Should the escape propulsion upper stage be guided or spin-stabilized?

The resolution of the latter, for example, is contingent upon mission and launch corridor considerations. Guided systems incorporate a complete guidance package and active reaction control and are employed on missions where good aim point accuracy is required. Spin-stabilized upper stages, on the other hand, provide a means of achieving maximum ΔV but with degraded pointing accuracy. In order to minimize the effects of thrust misalignment, and to capitalize on the guidance capability of basement launch vehicles, spin-stabilized powered spacecraft configurations would be guide-spun in a spin table prior to upper-stage ignition. Even with these precautionary measures, dispersions on the order of 1 deg minimum are probable.

For direct flights for which there are no stringent launch corridors, the spin-stabilized configuration with a nominal spacecraft attitude control system may be adequate. For the Jupiter swingby alternate, the aim point accuracy requirements are more severe but do not necessarily place excessive demands on the spacecraft midcourse maneuver system to effect the necessary corrective maneuvers. In selecting the course corrective maneuver system, a comparison must be made of gas dynamic thrusters as opposed to electric propulsion systems. Because of the sustained nature of reaction control offered by the latter, electric propulsion systems, such as ion and colloid thrusters, may be superior to gas dynamic systems from the standpoint of weight.

To facilitate the resolution of the staged solid propulsion system requirements, a large body of parametric data was subsequently generated, and analyses were performed. Various design options available were assessed on the basis of state-of-the-art and advanced propulsion performance capabilities estimated. By evaluating the performance outputs on the basis of tailored spacecraft propulsion motors, the maximum performance envelope per payload weight can be established.

To this end, solid motor characteristics for both state-of-the-art and advanced technology propulsion system capabilities have been defined and/or estimated and their performance data compiled. Typical performance data utilized during the conduct of the study are given in Table 4.

In the parametric performance analyses, described later in the report, the mass fractions of the state-of-the-art motors and the advanced technology motors were lowered by 0.045 to 0.885 and 0.91, respectively, to account for interstage structural weight and guidance and control weight. Late in the study, when a new multi-stage propulsion concept using the innovative "conesphere motor" (see Appendix A) arose, motor mass fraction was not determined because only the stage mass fraction was found to be meaningful; the guidance and control weight was, of course, included in its stage weight to keep the comparison on an equal basis.

To minimize the costs of solid propulsion stage development and flight hardware delivery, a developmental method utilizing scaling laws is advocated. In this approach, the smallest stage would be extensively investigated and developed to establish the integrity of the basic design. All subsequent stages would then be linearly scaled from the smallest unit, thereby realizing a significant savings on the costs of development and flight hardware delivery. This developmental scheme is by no means an innovation -- its rudiments can be traced to earlier solid motor test programs (Ref. 1).

By adopting this developmental approach, a savings on the order of 70% has been estimated for a four-stage 10,600-kg (23,500-lb$_m$) spacecraft propulsion system (Ref. 2) as opposed to those costs associated with conventional developmental techniques. Thus, in contrast to the employment of existing single-stage non-optimum motors or the probable use of multiple non-optimum stages, this approach renders the development of tailored solid upper stages a cost-competitive venture. Moreover, assuming the high-mass-fraction conesphere motor development (Appendix A) proves successful, stage mass fractions on the order of 0.935 would be technically feasible. These advances, in comparison with the advanced propulsion technology capabilities predicted for conventional designs (Table 4), can be expected to have a significant impact upon the gross stage weight (e.g., on the order of 1435 kg (3163 lb$_m$) for a typical Jupiter swingby mission) and greatly enhance the overall mission/spacecraft capabilities.

C.   Launch Vehicle Considerations

In order to minimize the monetary impact of basement launch vehicles, the list of candidate designs was limited to existing and projected intermediate-sized vehicles. For this study, the basic launch vehicle performance data given in the OSSA Launch Vehicle Estimating Factors Handbook (Ref. 3) were used as the basis of performance evaluation. Data given for existing launch vehicles were checked against those supplied by the launch vehicle contractors and basic users. Load factors, fairings, and other constraints were similarly determined and found to be compatible with other available data.

To facilitate the feasibility assessment of candidate propulsion system designs, a 16% decrement in payload lift capability was assumed to accommodate anticipated mission-peculiar weight assignments such as inert support structures (e.g., spin table, increased weight of interstage adaptors, launch guidance inerts), launch window constraints, and the like. Thus the lift capabilities determined were representative of useful payloads assessed to the powered spacecraft.

The inadequacies of existing launch vehicles were indicated earlier in conjunction with the discussion of Fig. 2. In ensuing discussions, the inadequacies or marginality of incorporating state-of-the-art propulsion technology in the upper stages will also be delineated (Section VA3).

V. PROPULSIVE PERFORMANCE EVALUATION

A. Solar System Escape

1. **Parametric Analyses.** Parametric data characterizing the performance capabilities of the spacecraft escape propulsion system were generated to serve as the basis for subsequent tradeoff studies. Figure 5 shows the ratios of initial mass of the powered spacecraft to its payload (i.e., spacecraft) mass as a function of the total velocity increment ΔV provided by the solid stages, and the number of stages. The curves are normalized with respect to launch vehicle mass and are representative of a family of similar curves produced by varying the specific impulse and mass fraction of the stages.

To facilitate the conduct of tradeoff studies and to identify critical propulsion parameters, influence coefficients were formulated. The utility of influence coefficients constructed during the course of the study is illustrated in Table 5, where the effects of variations of independent variables such as propulsion payload mass M_{PL}, total velocity increment V, specific impulse I_{sp}, staging factor S (i.e., the reciprocal of 1 minus the stage mass fraction), and number of stages n on powered spacecraft mass M_0 are tabulated for a selected number of stages. Influence coefficients with large negative numbers are most desirable; these imply significant reductions in gross stage weight with slight improvements in independent variables. The effect of stage number, for example, is rather pronounced but drops markedly with increasing stage number. Hence, the more probable range of n is expected to vary from ~3 to 5 in order to maximize the influence of this independent variable.

The other single most influential parameter appears to be the staging factor, which is directly correlatable to stage mass fraction. Note that, unlike the stage number, the effect of the staging factor is relatively pronounced over a wide range of stage number. It follows then that the development of high-mass-fraction motors offers promise of a major improvement in mission performance capability.

The effect of I_{sp} is also important, but its measure is not as significant as that of n or S.

The sensitivity of spacecraft performance to stage mass fraction was also computed to evaluate the significance of employing advanced propulsion systems, such as the conesphere concepts (Appendix A), on transit time to 40 AU and payload. Figure 6 indicates the results when the launch vehicle is a TITAN IIIC with a weight M_0 in 185-km (100-nm) orbit of 10,669 kg (23,520 lb_m), for a spacecraft with four stages of spacecraft propulsion and a propellant specific impulse of 3001 Ns/kg (306 lb_f-s/lb_m).

Transit times for direct flights range from about 19 years for a stage mass fraction of 0.86 down to about 11.9 years for a stage mass fraction of 0.96 when the spacecraft weight is held constant at 272.2 kg (600 lb_m). If these times prove to be too long, Jupiter swingby missions could shorten them by several years. Of course, the spacecraft must then be attitude-stabilized with a capability for midcourse corrections.

The payloads in Fig. 6 are of interest for three specific cases--all for a fixed transit time of 13.4 years. If state-of-the-art motors (without the conesphere concept) were used, the stage mass fraction would be 0.885 and the permissible payload 229.1 kg (505 lb_m)--well below the 272.2 kg (600 lb_m) believed to be the minimum meaningful payload. If, alternately, the conesphere concept and the carbon composites were used with only minor advancements in technology, the mass fraction would become 0.907 and the payload would rise to 272.2 kg (600 lb_m), the estimated minimum.

Finally, if the advanced all-carbon composite technology could be used in the conesphere, then the resultant stage mass fraction of 0.935 would increase the payload to 318.9 kg (703 lb_m). It has been estimated that the 46.7 kg (102 lb_m) increase in payload would approximately double the scientific worth of the mission. It is of interest to note that there is growth potential in the design to increase the stage mass fraction above 0.935. In other words, the designs evaluated are believed to be realistic and may prove to be even better than indicated.

Figure 7 shows the effect of stage mass fraction on transit time to 40 AU and on payload when the shuttle is the launch vehicle with an M_0 in 185-km (100-nm) earth orbit of about 24,720 kg (54,500 lb_m). Transit times for direct flight and a 272.2-kg (600-lb_m) spacecraft are quite reasonable, ranging from 11.5 down to 9.3 years. Payloads, as would be expected, are more sensitive than for the TITAN III, increasing from 272.2 kg for a stage

mass fraction of 0.91 to 338.8 kg (747 lb$_m$) for a mass fraction of 0.935. The latter shows a payload increase of 58% over the 214.1-kg payload with motors based on today's state-of-the-art.

2. Launch Vehicle Selection. In assessing the applicability of candidate launch vehicles, an initial screening of basement launch vehicles was conducted assuming a 185-km (100-nm) orbital start. Launch vehicles considered in the analysis included Titan IIIB, Titan IIIC, and Titan IIID. (Both the five- and seven-segment versions of the Titan IIIC and Titan IIID were considered.) Upper stages included in the study were Centaur, stretched Centaur, fluorinated Centaur, VUS, Burner II (2300), and TE 364. The shuttle was also considered as a candidate basement launch vehicle.

Table 6 presents a compilation of C_3 exceedances of solar escape for the various candidate launch vehicle/upper-stage assemblies considered for payload weights of 272 and 408 kg (600 and 900 lb$_m$). Also shown is the launch vehicles' capability without the staged solid upper stages. Note that several launch vehicles can provide for solar system escape without the solid stages when the solid-stage mass fractions are 0.91. The tabulation is also useful in determining crossover points (for the more energetic launch vehicles) at which gains in C_3 justify the employment of an upper stage. For example, for the TIIID/Centaur (F)/VUS launch vehicle boosting a 272-kg (600-lb$_m$) payload, the crossover point occurs at the employment of a five- or six-motor upper stage. Conversely, a gain in the employment of an upper stage on the TIIID (7)/Centaur (F)/VUS is never realized, even for spacecraft utilizing eight solid upper stages.

A representative plot of C_3 output as a function of number of upper stages and payload mass is presented in Fig. 8 for a Titan IIID (7)/Centaur/ VUS launch vehicle. These data are based upon a 185-km (100-nm) orbital start with advanced technology propulsion performance capability (i.e., solid motor stage mass fractions of 0.91). Note that the solar system escape threshold is readily exceeded for all reasonable values of stage number for payload weights ranging between 272 and 408 kg (600 and 900 lb$_m$)--values corresponding to the probable range of spacecraft weight.

Comparative data relating the propulsive performance characteristics of the space shuttle system were also generated assuming a 272-kg (600-lb$_m$) payload, 185-km (100-nm) orbital start, and advanced technology propulsion

capabilities. The results of this exercise are tabulated in parametric form (Table 7). The corresponding plot of C_3 output as a function of gross upper-stage weight and stage number is presented in Fig. 9. Note that the C_3 energy level for solar system escape can be readily achieved over a wide range of probable stage numbers. Additionally, the C_3 level corresponding to direct flights (i.e., $C_3 = 250$) is also within reach of the 27,000-kg (59,000-lb$_m$) payload lift capability being assumed for one configuration of the space shuttle system (Ref. 4) for powered spacecraft whose stage numbers are in excess of three.

3.   Spacecraft Escape Propulsion System. The stage weight breakdown of representative solid upper stages was estimated, and the characteristics formulated for a typical four-stage spin-stabilized powered spacecraft configuration are presented in Table 8. Weight estimates made for a representative four-stage powered spacecraft configuration are tabulated against comparable subsystem weight assignments realized on Burner II designs in order to demonstrate the credibility of our assumptions. As noted in the table, the spacecraft escape propulsion system is without a guidance and autopilot package and an attitude control system. However, a tracking and telemetry capability is retained by which the upper stage can relay propulsion system measurements to the ground station. Propulsive performance capabilities denoted are based upon advanced technology propulsion properties estimated for aluminized solid propellant motors. Throughout the study, an assumption was made that the propulsive characteristics of each stage were identical and that each stage contributed an equal velocity increment so as to facilitate the determination of optimum staged vehicle design configurations.

The most promising launch vehicle/spacecraft escape propulsion system assembly underwent a further staging velocity optimization study. Results of this study for a representative Titan IIID (7)/Centaur family launch vehicle with a four-stage upper stage and 272-kg payload is depicted in Fig. 10. Here, the staging velocity plotted on the abscissa is synonomous with basement launch vehicle burnout velocity. With the use of state-of-the-art propulsive capability, the vis-viva energy level output falls short of achieving the program goal of $C_3 = 250$ for direct flights. Contrarily with the use of advanced technology propulsive capability in the upper stage, it is possible to exceed the C_3 output goal over a wide range of staging velocities varying from

16

~10-15 km/s. Moreover, because of the wide range over which C_3 exceeds the program goal, it is possible that the spacecraft designer may be able to judiciously select operational conditions to obviate upgrading the structural integrity of existing launch vehicles. For example, selecting the staging velocities in excess of 14.2 km/s (corresponding to the base loading structural threshold) for the Titan IIID (7)/Centaur (STR)/BII (2300) launch vehicle used in Fig. 10 eliminates the necessity for a very expensive redevelopment and requalification program on the existing launch vehicle.

A similar comparison of the most probable basement launch vehicles was made for both the baseline and alternate missions. The conditions for maximum C_3 output are summarized in Tables 9 and 10 for the direct flights and the Jupiter swingby alternate missions, respectively. It should be noted that in each instance, there is some margin in launch energy with which to exploit payload weight and/or sophistication vs. time/distance traversed in future tradeoff studies.

4.   Cost Analysis. Cost data associated with the development and delivery of flight hardware solid motors were also generated (Fig. 11). Assumptions used to develop these data are summarized below:

1.   Technology advancement or programs with a large number of motors (curve I)

   a.   Programs are based on previous cost calculations of motors where programs were stretched out in time or where specifications changed during the program.

   b.   Documentation requirements are unusually great.

   c.   Flight motor and spares (4 to 8) are delivered. For purposes of this study, the costs associated with this family of curves were assumed applicable for the development of the advanced technology propulsion capability motors being evaluated.

2.   Modified motor or scaled motor program (curve II)

   a.   Qualification program is small: five static test firings, three at AEDC.

   b.   One inert and three flight motors are delivered.

c. Twelve to 18 months delivery for motors 907 kg (2000 lb_m) or less; 18 to 24 months delivery for larger sizes.

d. No significant motor specification changes are assumed after contract start.

e. Program includes typical temperature-cycling tests of motors and firing at extreme temperatures at AEDC, and spin balancing for motors where required.

f. Program does not include testing in a radiation environment, thermal soak in vacuum chamber or other elaborate testing, documentation, and program stretchout.

3. Production motor costs (curve III)

a. Limited order of 5 to 10 motors is delivered.

b. Costs are based on industry's past responses to RFQ.

c. No TVC or thrust termination is required.

d. Spherical or short cylindrical section motor using titanium cases is assumed.

e. High-expansion-ratio nozzles are employed for vacuum operation.

f. Costs are in 1971 dollars.

Upper-stage cost data as a function of number of upper stages were generated for the anticipated range of gross stage weights and the results plotted in Fig. 12. Note that the curves are relatively flat in each instance and approach an asymptote rather quickly within the range of probable stage numbers anticipated. Note also that this trend (cost-insensitivity) becomes even more pronounced with increasing gross stage weight. Hence, as these costs are added to those associated with the basement launch vehicle(s) and mission-peculiar engineering and hardware costs, the effect of stage number can be expected to play a diminishing role in dictating an optimum cost-effectiveness configuration in the higher-energy missions.

Costs associated with the standard basement launch vehicles were extracted from Ref. 5. Corresponding costs of projected launch vehicles were generated in terms of hardware and prorated annual support/launch costs and the related needs for mission-peculiar engineering and hardware

costs reflected. A summary of the recurring and nonrecurring costs estimated for the most promising basement vehicle assemblies is presented in Table 11. All basement vehicles are assumed to be in existence, and the nonrecurring costs are those associated with engineering and hardware costs for the first-of-a-kind mission integration only. The space shuttle system, however, is assumed to be uniquely burdened with amortized development costs that are included in the nonrecurring cost column. Allowances are made in the support portion of the recurring costs to include nonpropulsive subsystems such as shroud, guidance, adaptors, and spin tables.

5. _Effectiveness Measure._ To interrelate the propulsive performance and the accomplishment of the scientific mission, an effectiveness measure criterion was established. This criterion, mission worth, identifies the increase of the scientific value of the mission with payload weight (e.g., increased number of instruments) and with distance traveled from the sun. A preliminary estimate of how the mission worth for the baseline science package might vary with distance was made; the results are presented in Fig. 13. These are very preliminary measures of mission worth which most scientists object to making; however, the worth estimates are useful in that they allow optimization of payload and launch energy levels.

From Fig. 13 and other mission data, a plot was constructed to relate mission worth as a function of flight time for the C_3 levels corresponding to direct flights and Jupiter swingby missions (Fig. 14).

6. _Reliability Assessment._ An estimate of the reliability characteristics of representative spacecraft was made for the direct and swingby alternate Jupiter missions (Figs. 15 and 16) by scaling comparable data generated for the Grand Tour flights (Ref. 6). Here, the probability of success in performing the basement vehicle operation is assumed to be 1.0. The deviations between stage numbers were also estimated based upon inherent reliability properties of large solid propellant motors (without thrust vector control) reported in NASA-sponsored Failure Warning and Motor Malfunction Studies (Refs. 7 and 8). It is important to note that the differences in reliability among candidate systems (i.e., systems of differing stage number) diminish as greater reliability is achieved. Hence, for long-term missions with equivalent performance alternates, reliability becomes a less significant factor in candidate design selection. Conversely, for

systems of differing performance equivalence (e.g., vis-viva energy level, mission time, etc.), the differences can be expected to have a significant impact upon the overall cost-effectiveness rating of the various competing systems.

7. Cost-Effectiveness Assessment. The comparisons of candidate designs on the basis of either performance, cost, or reliability individually do not provide sufficient information to determine the competitive position of the various design options. Cost-effectiveness techniques, however, provide a means for combining these three parameters into a single variable, and allow the determination of the design's relative merits based on a single parameter (Ref. 9). In addition, the technique provides a means for determining the relative importance of performance, cost, and reliability inputs.

Cost effectiveness, defined as expected mission return for dollar expended, is expressed as follows:

$$CE = \frac{PW}{C_T}$$

where

P = spacecraft probability of success

W = mission worth

C_T = total mission cost

Using the above expression and the parametric data developed, a cost-effectiveness assessment of the various candidate designs was made for select design "hard points" capable of effecting the direct and swingby missions. The results of this assessment are summarized in Table 12 for varying stage numbers ranging from 3 to 5.

Note that the cost-effectiveness ratings of the various systems appear to peak at n ≤ 4, and that the candidate systems available for the Jupiter swingby mission all proved superior to the most competitive direct flight options evaluated. Additionally, there are a few intermediate-sized basement vehicles capable of performing the identical Jupiter swingby mission at a much higher cost-effectiveness rating than the space shuttle system. Notably, the most cost effective system will be one that utilizes the Titan IIID (7) as the

basement vehicle, followed by the Titan IIID, space shuttle, Titan IIIC (7), and lastly, the Titan IIIC launch vehicle. The space shuttle system, because of the great uncertainty associated with determining realistic recurring and nonrecurring costs and deliverable payload, cannot as yet be properly assessed.

In direct flights involving the employment of launch vehicle assemblies, the rating of the space shuttle system fared somewhat better (second). However, if the projected costs associated with the space shuttle system lean toward the high end of the anticipated cost range (as speculated by most spacecraft engineers), its relative ranking could be further suppressed. Although the assessment was conducted over a limited range of stage number, the trends established are believed to be valid and representative over a wider stage number spectrum. Assuming functional equivalence, for configurations of increasing stage number, the reliability rating drops correspondingly, accompanied by a diminishing cost differential. At the lower end of the scale, although the reliability rating of the overall vehicle increases with decreasing stage number, its effect is more than offset by escalating stage weight (as evidenced by the influence coefficients) and hence, rising costs. Therefore, the occurrence of cost-effectiveness maxima between stage numbers of 3 and 4 appears highly plausible.

Additional expository remarks, along with a typical example of a cost effectiveness assessment computation, are presented in Appendix B.

B. Out-of-Ecliptic Capability

The out-of-ecliptic capability of the most promising launch vehicles was evaluated to assess the versatility of adapting the staged solid approach to other types of high-energy missions. The celestial latitudes and displacements achievable were estimated on the basis of their maximum C_3 output, and the results are summarized in Table 13. For each candidate launch vehicle, the characteristic velocity V_c corresponding to the maximum vis-viva energy output is tabulated along with probable ranges of celestial latitude displacement, radial distance from the sun, and possible mission flight times. All performance predictions listed are based on a four-stage powered spacecraft configuration, 272-kg (600-lb_m) payload, and advanced technology propulsion capability predictions. The range of out-of-ecliptic mission profiles listed represents the maximum celestial latitude accessible within the

normal azimuth limits from the Eastern Test Range for nominal direct out-of-ecliptic mission flights and the corresponding celestial latitude possible at a 10 AU radial distance from the sun.

As noted in Table 13, for launch vehicle assemblies that are relegated to Jupiter swingby baseline missions, the maximum celestial latitudes possible for direct out-of-ecliptic probes range from 25.5 to 28.6 deg. For direct flight baseline configurations, the out-of-ecliptic capability rises to 32 deg minimum. Further, by negotiating a Jupiter swingby maneuver, celestial latitudes in excess of 84 deg are within the realm of capability (although the trajectories will be more elliptic) for each of the candidate launch vehicle assemblies listed.

C.   Comparison with Alternates

Summarizing the previous discussion, the powered spacecraft concept utilizing staged solids offers the advantages of achieving early, low-cost solar escape missions with high reliability. For direct flights, a penalty is paid in the degradation of spacecraft design sophistication owing to the propulsive system weight assignment that detracts from the "useful" payload. However, these flights are detached from any celestial mechanics constraints and provide more flexibility in the launch mode.

The Jupiter swingby alternate has the advantages of achieving an equivalent mission with significant reduction in propulsive system weight assignment. However, because of celestial mechanics constraints and the Jovian environment, penalties are attached. For example, to acquire the regions of scientific interest in the flight times specified, launch window and launch year constraints are imposed. (Launch window constraints, however, are not considered excessive inasmuch as favorable alignment of Jupiter occurs in ~13-month intervals.) In addition, to negotiate a successful swingby encounter, added corrective maneuver capabilities and/or vectoring accuracy are required (in comparison with direct flights). Uncertainties in the Jovian radiation model (both flux and energy levels) and encounter geometry further detract from the mission return.

Because of exposure to the radiation environment at high fluence levels, a permanent degradation in transmitted data is anticipated, and little improvement is expected beyond Jupiter swingby. Although the addition of shielding should offer some degree of protection against the low-energy particles, it is

questionable whether any significant retardation of electrons or protons at the higher fluence levels can be expected. The only alternative then is to increase the altitude of closest approach and absorb a loss in gravity assist. Since there is little restraint on the permissible escape corridor beyond the swingby, a post-engagement corrective maneuver capability is not a requirement.

By implementing these missions with solid propulsion stages, the program goals of low cost and high reliability are readily achieved. There are, of course, several alternate propulsive systems whose performance output meets or far exceeds the mission requirements established. Among them are liquid propulsion and solar electric propulsion (SEP) systems. Each of these alternate propulsion systems has unique capabilities (e.g., the liquids typically exhibit high flexibility and high I_{sp}, whereas the SEP is especially suitable for three-axis stabilized spacecraft and inherently exhibits superior vectoring accuracy), and hence, is expected to be uniquely suitable to a given class of mission. With the advent of more advanced scientific missions in which added flexibility and/or vectoring accuracy becomes an increasing requirement, the liquids are expected to surpass the solids, SEP to surpass the liquids, nuclear electric propulsion to surpass SEP, etc.

Ground rules adopted for the study were selected on the basis of reaching the outer fringes of the solar system in a time frame coincident with sustaining public and scientific interest and within the lifetime of spacecraft hardware. Simply probing the regions selected at distances appreciably less than 40 AU in a comparable time frame would not materially add to the knowledge acquirable by Pioneer class or Outer Planets Project flights (although these flights could readily be accomplished by existing vehicles and without the need of a powered upper stage). With Jupiter swingby, the Pioneer spacecraft is capable of solar system escape. However, the on-board propellant supply available to maintain earth lock limits the probable range of telecommunications to a maximum of 12-15 AU.

Outer Planets Project missions can traverse much larger distances, and the minimum science package associated with the one proposed configuration is capable of performing fields and particles as well as planetology experiments. Because of this capability mix, it is difficult to assess the relative cost-effectiveness ratings between the baseline mission and a typical Outer

Planets Project flight. Although the mission return from the latter is substantial, the increase in program costs and celestial mechanics constraints is correspondingly pronounced. A basis of equivalence would be a difficult criterion to formulate and was not attempted within the scope of this study.

The only meaningful method of comparison between the baseline configuration and alternate propulsive system approaches would be on the basis of functional equivalence. Inherent properties of the alternate approaches do not necessarily lend themselves to this basis of comparison. As previously noted, SEP is characteristically associated with a three-axis-stabilized spacecraft with relatively large and complex payloads (net spacecraft mass approximately 400 kg or larger). The baseline configuration, on the other hand, is typical of a smaller, spin-stabilized class of spacecraft, similar to the Pioneer. Because of the basic differences in the carrier and their mode of operation, a significant difference in spacecraft capabilities, requirements, and weights is anticipated. Although both the direct and gravity-assist missions are within the performance capability of the SEP, the Jupiter swingby alternate may be the most viable option because of the exceptional savings in propulsive system weight.

More recently, the feasibility of a spin-stabilized SEP was postulated (Ref. 10) for a similar outbound mission. In this study, it was concluded that although the loss in power output may be as large as 30%, the spin-stabilized configuration would be cost-effective. Weight savings realized from the elimination of the thrust vector control mechanism for the spin-stabilized version were offset by the weight assignment for the additional solar array; however, it was generally concluded that the spin-stabilized version would be lighter, cheaper, and more reliable than the more complex three-axis-stabilized system.

The spacecraft application of a solar electric propulsion system encounters new problems of configuration. These problems have been studied extensively, and feasible solutions have been found (Refs. 11 and 12). Basic to the configuration is the deployment of a large-area solar array oriented toward the sun. In addition, the low-thrust ion engines must operate for long periods of time, and care must be taken that the exhaust does not interact with other on-board systems.

D. Growth Options

The existing propulsive energy margins of the most promising launch vehicle assemblies are expected to adequately accommodate small perturbations in ground-rule constraints as well as to provide a limited margin for evolutionary growth. However, as the ground rules and mission requirements become more demanding, alternate propulsion systems, basement vehicles, and spacecraft approaches must be examined and their impact on the resulting conclusions evaluated.

Potential growth options include application to solar probes, comet and asteroid rendezvous, and outer planetary probe missions. The latter application includes the possibility of utilizing a dual-mode operational spacecraft capable of traversing regions of lower scientific yield as a spinner and later activating a stable platform network to permit active imaging at the target planet. Alternately, the added payload weight margin may be dedicated to the delivery and deployment of subsatellites, landers, or planetary probes. Subsatellites, for example, could conceivably be employed to map the radiation belt about the target planet without actually penetrating the turbopause. Independent of the baseline design, any added weight assignment to the science package, data storage, or transmission modules should materially add to the complexity of scientific experiments that could be considered for missions to the outer fringes of the solar system.

To implement the more energetic mission growth options within a reasonable flight time, added propulsive capability is required. The extension of totally chemical basement launch vehicle capabilities is representative of the coupling of the Saturn V/Centaur assembly with a four-stage solid escape propulsion augmentation system. For spacecraft weights of 272, 408, and 680 kg (600, 900, and 1500 lb_m), vis-viva energy levels of 491, 442, and 382 km^2/s^2 are achievable. The significance of these C_3 energy levels is the realization of traversing distances as far as 100 AU in flight times on the order of 15.6 to 18.1 years. Alternately, assuming a 10-year lifetime, the spacecraft selected are capable of traversing 56 to 64 AU within that lifetime. Additionally, with these launch energies, the spacecraft would be capable of negotiating celestial latitudes of $\sim$41-48 deg on out-of-ecliptic direct flight missions.

Similarly, by incorporating solar electric propulsion and a four-stage solid chemical upper stage with the Saturn V/Centaur basement vehicle, the following equivalent launch energy levels are possible:

| Spacecraft Weight | | C_3 |
kg	(lb$_m$)	km^2/s^2
272	(600)	549
408	(900)	495
680	(1500)	429

With these vis-viva energy levels, it should be possible to further reduce trip times out to 100 AU to ~14.8 to 16.4 years. Conversely, with a 10-year lifetime, the identical spacecraft would be capable of traversing 61-67 AU minimum within their lifetimes. Celestial latitudes possible at these higher C_3 levels would be correspondingly higher (i.e., ~44-55 deg) for direct out-of-ecliptic missions.

E.   Future Tradeoffs

The effect of C_3 on mission flight time is illustrated in Fig. 17. At the solar escape threshold corresponding to a C_3 of 152 km^2/s^2 and with direct flight, it is possible to traverse distances out to 40 AU in flight times on the order of 19 years. With Jupiter swingby, the flight time is reduced to 8.3 years. With direct flight at a C_3 of 250, the corresponding flight time is reduced to 10.5 years, and with Jupiter swingby, to 6.3 years.

This plot was also useful in delineating major tradeoffs that must be conducted during the performance of the study. In addition to describing the propulsive requirements, it identifies the necessity to evaluate time of flight vs. distance vs. reliability vs. data management techniques. The interrelationships of these parameters are grossly summarized as follows. Reliability rating is a function of time of flight, weight (redundancy), and event occurrence. Telecommunications is dependent upon transmission frequency, data rate, distance, power, and, of course, the ability to maintain earth lock. Distance becomes an overriding parameter in maintaining transmission to the outer fringes of the solar system, simply because of transmission beam dispersion. Power for flights beyond Jupiter will undoubtedly rely upon RTG sources, whose system specific weight is estimated at ~70 kg/kW (154 lb/kW) for flight times on the order of 10 years. The output of these devices is time-dependent owing to the half-life properties of the nuclear power source. Additionally, a penalty is attached because of the remote isolation and/or shielding that must be provided in spacecraft installations employing RTG devices.

For flight times on the order of 10 years, a major portion of the overall project costs may be attributable to mission operational costs during flight. One method by which to impact these costs is through the use of sophisticated data management techniques, including on-board data preprocessing, thresholding, compression, and storage, as well as modulating the data transmission rate.

For example, the consensus of scientists interviewed was that the transmission rate of scientific data should only be suppressed to the real-time data rate threshold. Spacecraft designers, however, are of the opinion that the data rate can be further suppressed by significant proportions through the employment of on-board preprocessing techniques. Hence, the corresponding scientific data rates at 40 AU may vary from, say, 1 to 4 bps down to fractions of bps, depending upon the on-board capabilities incorporated. Therefore, for slight additions in spacecraft weight, large reductions in ground station dedication and use may be realized.

Although the engineering data rate may still be the overriding parameter, its frequency of occurrence and duration are not expected to be of sufficient magnitude to inflict any exhorbitant penalties or cause loss of scientific data. Storage and subsequent burst transmission options provide further means of circumventing this problem area. Notwithstanding, the incorporation of these and other data management innovations will have a significant impact upon spacecraft design, ground station dedication, and overall program costs.

In comparing the relative merits of direct flights and Jupiter swingbys, consideration must be given to weighting celestial mechanics constraints such as launch windows and launch years necessary to acquire the Lyman-alpha region and the sun's apex. Additionally, the extent and period of degradation in the particles and fields instruments due to the engagement of the hostile Jovian environment should be weighed against the benefits of gravity assist derived from the swingby. There is, however, some degree of inherent protection against the high proton density due to possible built-in shielding, uncertainties in the flux density, and field distribution. The pointing accuracy requirement for swingby acquisition becomes quite severe, but it is anticipated that the type of gravity-assist maneuver envisioned for these missions can be successfully negotiated through ground station tracking

and nominal on-board corrective maneuver capability ($\sim$20-50 and $\sim$170-200 m/s minimum total ΔV estimated, respectively, for guided and spin-stabilized escape propulsion augmentation systems). Since there is little criticality attached to the escape corridor beyond swingby encounter, a post-engagement corrective maneuver capability is not envisioned.

Ideally, the implementation of the powered spacecraft conceptual approach discussed in this report relies on the use of a simple, energetic propulsive system that is not severely hampered by launch windows or celestial mechanics constraints. However, in selecting a direct flight devoid of gravity assist, a penalty is paid in the degradation of sophistication assigned to the spacecraft or science package. Conversely, the Jupiter swingby alternate may represent a more nearly optimum tradeoff between guidance/vector delivery accuracy and science package/spacecraft sophistication or mission worth.

Of course, the launch window(s) have other far-reaching ramifications that affect the relative displacement of the magnetosphere, minimum launch energy, and hence, propellant weight. Moreover, as the vectoring accuracy requirements become more severe due to launch corridor constraints, solid propulsion systems become less attractive.

Although the bulk of these tradeoffs are outside of the scope of this study, they are mentioned in order to place the proper perspective on any future work.

VI. CONCLUSIONS AND RECOMMENDATIONS

The following basic conclusions have been derived from this study:

1. A class of missions of scientific significance (e.g., solar escape and extra-ecliptic probes) has been identified that could utilize a simple, energetic propulsion system.

2. A problem arises in that the performance of existing launch vehicles (as energetic as the Saturn V and shuttle-Centaur basement vehicles) and state-of-the-art motors is inadequate or marginal.

3. A solution has been offered in the form of tailored solid motor upper stages (powered spacecraft concept) developed to augment launch vehicle performance. This approach would be especially favorable if the new multistage concept based on the conesphere motor (Appendix A) were to be adopted.

4. The advantages of such a conceptual approach include low cost, high reliability, and reduced flight time.

5. The gross feasibility of adapting solid propulsion systems to the powered spacecraft concept has been demonstrated in conjunction with several existing and projected basement vehicles. These include the space shuttle, Titan, and Titan/Centaur family launch vehicles.

6. The Jupiter swingby alternate was judged to be a more cost-effective means of effecting solar escape than the direct-flight baseline mission.

7. Launch energy margins have been identified for each of the most promising designs in which the upgrading of spacecraft sophistication and mission worth can be exploited in future studies.

8. Advanced propulsion systems and alternate spacecraft approaches can be assessed for more advanced applications in which there is a need for accurate vector delivery requirement.

Based on work performed during the conduct of this study, several regions of high-yield payoff have been identified in which advanced technology

development efforts could be fruitfully directed at the present time, such as the development of unusually high mass fraction solid propellant motors.

VII. RECOMMENDED FUTURE WORK

To lend further credibility to the results derived, it is recommended that additional studies be conducted to verify the results to date and address currently unanswered questions. Specific recommendations for future work are as follows:

1. Perform an in-depth mission application study in which interdisciplinary inputs are provided to investigate the interactions of spacecraft propulsion (both chemical and electric), environmental constraints, data management, ground station dedication, spacecraft design, mission and operational requirements, etc., and their effects on mission performance and overall program costs.

2. Embody maturing technologies and mission data resulting from the Pioneer flights, Outer Planets Project, and related advanced technology development efforts to verify the conclusions drawn to date.

3. Exploit launch energy margins that may exist and upgrade the sophistication of the scientific missions that can be performed.

4. Evaluate the feasibility of alternate propulsive and spacecraft approaches to implement more sophisticated mission profiles. These approaches may entail the use of advanced liquid and electric propulsion systems or dual-mode operational spacecraft capable of extending the mission application potential to include solar probes, rendezvous, and outer planetary probes.

Table 1. Baseline typical science payload

Experiments	Weight, kg (lb$_m$)	Power, W
Helium vector magnetometer	2.2 (4.8) — 3.6 (8.0)	4.1 — 5.2
Plasma	2.7 (6.0) — 4.5 (10.0)	2.0 — 12.6
Cosmic ray	3.1 (6.8) — 4.5 (10.0)	2.2 — 5.0
Total	8.0 (17.6) — 12.6 (28.0)	8.3 — 22.8

Table 2. Additional science experiments

Experiments	Weight, kg (lb_m)	Power, W
Ac magnetometer	1.8 (4.0) − 3.2 (7.0)	3 − 5
Electron energy detector	2.7 (6.0) − 4.5 (10.0)	2 − 5
Lyman-alpha photometer	1.4 (3.0) − 3.2 (7.0)	3.5 − 5
Neutral particles	2.3 (5.0) − 7.3 (16.0)	1 − 3
Dust-particle detector	0.9 (2.0) − 2.3 (5.0)	0.7 − 2
Total	9.1 (20.0) − 20.5 (45.0)	10.2 − 20

Table 3. Spacecraft weight estimate

Subsystem/system	Mass, kg (lb$_m$)
Structure	46.3 (102) − 68.0 (150)
Communications	9.98 (22) − 16.8 (37)
Antennas	17.7 (39) − 20.4 (45)
Data handling	5.44 (12) − 15.9 (35)
Electrical power	64.0 (141) − 74.8 (165)
Electrical distribution	15.9 (35) − 18.1 (40)
Attitude control	14.1 (31) − 33.1 (73)
Propulsion (wet)	37.6 (83) − 64.4 (142)
Thermal control	5.90 (13) − 8.17 (18)
Balance weight	2.27 (5) − 4.08 (9)
Data storage	18.1 (40) − 25.0 (55)
Control computer subsystem	9.07 (20) − 19.1 (42)
Shielding	3.18 (7) − 7.26 (16)
Science payload	8.62 (19) − 33.1 (73)
Gross payload	258 (569) − 408 (900)

Table 4. Representative state-of-the-art and advanced
technology propulsion performance characteristics

State-of-the-art	Option 1	Option 2	Option 3
Motor weight, kg (lb_m)	90.7 (200)	453.6 (1000)	4536 (10,000)
Motor mass fraction	0.91	0.93	0.935
Vacuum specific impulse, Ns/kg (lb_f-s/lb_m)	2844 (290)	2903 (296)	2913 (297)
Stage mass fraction	--	0.885	--
Advanced technology propulsion prediction (performance prediction after 7 years R&D)			
Motor weight, Kg (lb_m)	90.7 (200)	453.6 (1000)	4536 (10,000)
Motor mass fraction	0.94	0.955	0.96
Vacuum specific impulse Ns/kg (lb_f-s/lb_m)	2942 (300)	3001 (306)	3011 (307)
Stage mass fraction	--	0.91	--
Advanced conesphere propulsion (see Appendix A)			
Vacuum specific impulse, Ns/kg(lb_f-s/lb_m)			3001 (306)
Stage mass fraction			0.935

Table 5. Propulsive performance influence coefficients

Number of stages	Influence coefficients				
	$\dfrac{\partial M_0}{\partial M_{PL}}$, kg/kg ($lb_m/lb_m$)	$\dfrac{\partial M_0}{\partial V}$, kg/mps ($lb_m/fps$)	$\dfrac{\partial M_0}{\partial I_{sp}}$, kg/s ($lb_m/s$)	$\dfrac{\partial M_0}{\partial S}$, kg/unit s ($lb_m/unit\ s$)	$\dfrac{\partial M_0}{\partial n}$, kg/stage ($lb_m/stage$)
3	112	14.9 (10.0)	-560 (-1236)	-3091 (-6816)	-9472 (-20880)
6	80.2	8.77 (5.89)	-329 (-726)	-1252 (-2760)	-844 (-1860)
9	74.7	7.86 (5.28)	-295 (-650)	-1002 (-2208)	-288 (-634)

Assumptions: $C_3 = 250\ km^2/s^2$, $M_{PL} = 272\ kg\ (600\ lb_m)$,

$I_{sp} = 3001\ Ns/kg\ (306\ lb_f\text{-}s/lb_m)$, $\mu_s = 0.91\ (\mu_p = 0.955)$.

Table 6. Vis-viva energy exceedances of solar escape for candidate launch vehicles employing aluminized propellant

Launch vehicle	C_3 max for M_{PL} = 272 kg (600 lb$_m$)[a]						C_3 max for M_{PL} = 408 kg (900 lb$_m$)[a]						$C_{3\,LV}$[b]	
	n = 3	4	5	6	7	8	n = 3	4	5	6	7	8	M_{PL} 272	408
TIIIB (STR CI + 2A3)/Centaur (F)						160								
TIIIB (STR CI + 2A3)/Centaur (F)/VUS						160								
TIIIC	170	178	182	185	187	188								
TIIIC/BII (2300)	182	191	196	200	202	203		158	161	164	165	166		
TIIIC/BE BII (1-BURN)	175	183	188	191	193	194			153	156	157	158		
TIIIC (7)	193	203	209	212	215	216	162	169	173	176	178	179		
TIIIC (7)/BII (2300)	175	183	188	191	193	194			153	156	157	158		
TIIIC (7)/BE BII (1-BURN)	182	191	196	200	202	203		158	161	164	165	166		
TIIID	169	177	181	184	186	187								
TIIID/Centaur	184	194	199	202	204	206	153	160	164	166	168	169		
TIIID/Centaur/VUS	175	183	188	191	193	194			153	156	157	158	169	158
TIIID/Centaur/TE 364 (2300)	184	194	199	202	204	206	153	160	164	166	168	169	164	
TIIID/Centaur/BII (2300)	184	194	199	202	204	206	153	160	164	166	168	169		
TIIID/Centaur (STR)/BII (2300)	184	194	199	202	204	206	153	160	164	166	168	169	158	
TIIID/Centaur (F)	177	186	191	194	196	197		153	156	158	160	161		
TIIID/Centaur (F)/VUS	177	186	191	194	196	197		153	156	158	160	161		
TIIID (7)	193	203	209	212	215	216	162	169	173	176	178	179	192	181
TIIID (7)/Centaur	208	220	226	230	233	235	177	185	190	193	195	196		
TIIID (7)/Centaur/VUS	180	189	193	196	199	200		155	159	161	162	163	194	184
TIIID (7)/Centaur/BII (2300)	184	194	199	202	204	206	153	160	164	166	168	169	173	159
TIIID (7)/Centaur (STR)/BII (2300)	184	194	199	202	204	206	153	160	164	166	168	169	184	171
TIIID (7)/Centaur (F)/VUS	182	191	196	200	202	203		158	161	164	165	166	220	210

[a] 185-km (100-nm) orbital start, I_{sp} = 3001 Ns/kg (306 lb$_f$-s$_3$/lb$_m$) μ_s = 0.91.
[b] Launch vehicle C_3 without additional upper stage(s).

Table 7. Maximum vis-viva energy levels of candidate solid
upper stages employing aluminized propellant
and launched from the space shuttle system
with a 272-kg (600-lb$_m$) payload

M_0, kg (lb$_m$)[a]	Number of stages								
	2	3	4	5	6	7	8	9	10
6804 (15000)	123	136	141	144	146	147	148	149	149
9072 (20000)	141	157	164	168	171	172	173	174	175
11340 (25000)	154	174	183	187	190	192	194	195	196
13608 (30000)	165	188	198	203	207	209	211	212	213
15876 (35000)	174	200	211	217	221	223	225	227	228
18144 (40000)	182	211	223	229	233	236	238	240	241
20412 (45000)	189	220	233	240	245	248	250	251	253
22680 (50000)	195	228	242	250	255	258	260	262	263
24948 (55000)	200	236	251	256	264	267	270	272	273
27216 (60000)	205	242	258	267	272	276	279	281	282
29484 (65000)	209	249	266	275	280	284	287	289	290
31752 (70000)	213	254	272	282	288	292	294	297	298

[a]M_0 = gross upper-stage weight (powered spacecraft weight).

Table 8. Upper-stage weight breakdown

Item	Stage		
	Burner II (1440) TE-M-364-2, kg (lb$_m$)	Burner II (2330) TE-M-363-4, kg (lb$_m$)	Powered spacecraft[a] four-stage, kg (lb$_m$)
Propulsion	63 (138)	67 (148)	355 (782)
Structure	28 (61)	40 (88)	375[b] (826)
Guidance and autopilot	16 (35)	16 (35)	0 (0)
Electrical	15 (34)	15 (34)	32 (70)
Attitude control	50 (110)	49 (108)	0 (0)
Tracking	11 (25)	11 (25)	11[c] (25)
Telemetry	4 (8)	4 (8)	4[c] (8)
Residuals/expendables	1 (3)	8 (17)	0 (0)
Total inert weight	188 (414)	210 (463)	777 (1711)
Impulse propellant	653 (1440)	1139 (2300)	7528[d] (16,597)
Mass fraction	0.78	0.84	0.91
I_{sp}, Ns/kg (lb$_m$)	2834 (289)	2775 (283)	3001 (306)

[a] 272-kg (600-lb$_m$) payload and 8.75-km/s (28,719-fps) ΔV_T assumed.
[b] Scaled from Burner II.
[c] For top upper stage only.
[d] Propulsive mass fraction = 0.955.

Table 9. Staging velocity optimization for direct solar system escape flights

Launch vehicle performance	Number of stages		
	3	4	5
TIIID/Centaur (F)/VUS			
C_3 max, km^2/s^2	259.5	261.3	262.3
V_c, km/s (fps)	14.63 (48000)	14.63 (48000)	14.63 (48000)
M_0, kg (lb_m)	1726 (3806)	1726 (3806)	1726 (3806)
TIIID (7)/Centaur/VUS			
C_3 max, km^2/s^2	265.8	267.3	268.4
V_c, km/s (fps)	15.24 (50000)	15.24 (50000)	14.02 (46000)
M_0, kg (lb_m)	1447 (3191)	1447 (3191)	2313 (5098)
TIIID (7)/Centaur (STR)/BII (2300)			
C_3 max, km^2/s^2	251.6	255.6	258.6
V_c, km/s (fps)	13.41 (44000)	11.58 (38000)	11.58 (38000)
M_0, kg (lb_m)	2586 (5702)	5409 (11924)	5409 (11924)
TIIID (7)/Centaur (F)/VUS			
C_3 max, km^2/s^2	289.5	291.6	292.7
V_c, km/s (fps)	15.24 (50000)	15.24 (50000)	15.24 (50000)
M_0, kg (lb_m)	1829 (4031)	1829 (4031)	1829 (4031)

Assumptions: M_{PL} = 272 kg (600 lb_m), I_{sp} = 3001 Ns/kg (306 lb_f-s/lb_m), μ_s = 0.91.

Table 10. Staging velocity optimization for Jupiter swingby missions

Launch vehicle performance	Number of upper stages		
	3	4	5
TIIIC			
C_3 max, km^2/s^2	172.5	179.2	182.8
V_c, km/s (fps)	8.53 (28000)	8.53 (28000)	8.53 (28000)
M_0, kg (lb_m)	8017 (17675)	8017 (17675)	8017 (17675)
TIIIC (7)			
C_3 max, km^2/s^2	197.3	205.0	209.7
V_c, km/s (fps)	9.14 (30000)	8.53 (28000)	8.53 (28000)
M_0, kg (lb_m)	8375 (18464)	10839 (23896)	10839 (23896)
TIIID			
C_3 max, km^2/s^2	169.6	177.2	181.4
V_c, km/s (fps)	8.53 (28000)	7.92 (26000)	7.92 (26000)
M_0, kg (lb_m)	7728 (17037)	10062 (22182)	10062 (22182)
TIIID (7)			
C_3 max, km^2/s^2	193.2	203.1	208.5
V_c, km/s (fps)	7.92 (26000)	7.92 (26000)	7.92 (26000)
M_0, kg (lb_m)	13679 (30157)	13679 (30157)	13679 (30157)

Assumptions: M_{PL} = 272 kg (600 lb_m), I_{sp} = 3001 Ns/kg (306 lb_f-s/lb_m), μ_s = 0.91.

Table 11. Cost estimate of representative basement vehicle assemblies

Basement vehicle[a]	Nonrecurring costs,[b] $ millions	Recurring costs		Total, $ millions
		Hardware, $ millions	Support,[c] $ millions	
T III C	1.20	15.69	6.34	22.03
T III C (7)	1.20	15.77	7.42	23.19
T III D	1.20	12.29	4.82	17.11
T III D (7)	1.20	13.08	5.19	18.27
Space shuttle[d,e]	12.40	-	-	<10.00
T III D (7)/Centaur(F)/VUS	1.20	23.16	9.85	33.01
T III D (7)/Centaur(STR)/B II (2300)	1.20	20.06	8.55	28.61
T III D (7)/Centaur/VUS	1.20	22.34	9.67	32.01
T III D/Centaur(F)/VUS	1.20	21.23	10.21	31.44

Assumptions: [a]All listed basement vehicles exist, and their development costs have been amortized.
[b]Mission-peculiar engineering and hardware cost for first flight only.
[c]Includes related costs of shroud, guidance, and adaptors.
[d]Space shuttle is uniquely burdened with amortized development costs.
[e]Based on private communications with North American Aviation, Inc. These data were selected because they were believed to be conservative or were expected to yield a more favorable position for the space shuttle.

Table 12. Cost-effectiveness assessment of candidate launch vehicle systems

Basement vehicles	Cost-effectiveness rating (probability of success × mission worth/$M)		
	n = 3	n = 4	n = 5
Jupiter swingby			
TIIID (7)	0.029764	0.029736	0.029465
TIIID	0.029761	0.029729	0.029468
Space shuttle	0.028941	0.028917	0.028785
TIIIC (7)	0.028581	0.028526	0.028259
TIIIC	0.028549	0.028492	0.028256
Direct			
TIIID (7)/Centaur (F)/VUS	0.024570	0.024481	0.024231
Space shuttle	0.024314	0.024425	0.024260
TIIID (7)/Centaur (STR)/BII (2300)	0.023980	0.023931	0.023686
TIIID (7)/Centaur/VUS	0.023961	0.023857	0.023613
TIIID/Centaur (F)/VUS	0.023859	0.023640	0.023412

Table 13. Out-of-ecliptic capabilities for most
cost-effective launch vehicles

Basement vehicle	C_3 max, km^2/s^2	V_c, km/s (fps)	Celestial latitude, deg	Radial distance from sun, AU	Flight time, days
TIIIC	179.2	17.33 (56854)	26.5 6.0	0.83 10.0	88 1300
TIIIC (7)	205.0	18.06 (59250)	28.6 8.0	0.81 10.0	87 1200
TIIID	177.2	17.27 (56662)	26.5 6.0	0.83 10.0	88 1200
TIIID (7)	203.1	18.01 (59075)	28.5 8.0	0.81 10.0	87 1200
Space shuttle (Jupiter swingby configuration)	164.2	16.89 (55421)	25.5 5.0	0.87 10.0	88 1250
TIIID/Centaur (F)/VUS	261.3	19.56 (64160)	32.6 12.0	0.78 10.0	87 1100
TIIID (7)/Centaur (STR)/BII (2300)	255.6	19.41 (63677)	32.3 11.6	0.78 10.0	85 1000
TIIID (7)/Centaur/VUS	267.3	19.71 (64658)	33.0 12.0	0.77 10.0	87 1050
TIIID (7)/Centaur (F)/VUS	291.6	20.31 (66649)	35.0 13.8	0.71 10.0	85 1000
Space shuttle (direct flight configuration)	265.6	19.66 (64516)	33.0 12.0	0.77 10.0	87 1050

Assumptions: Four-stage powered spacecraft, M_{PL} = 272 kg (600 lb$_m$), I_{sp} = 3001 Ns/kg (306 lb$_f$-s/lb$_m$), μ_s = 0.91.
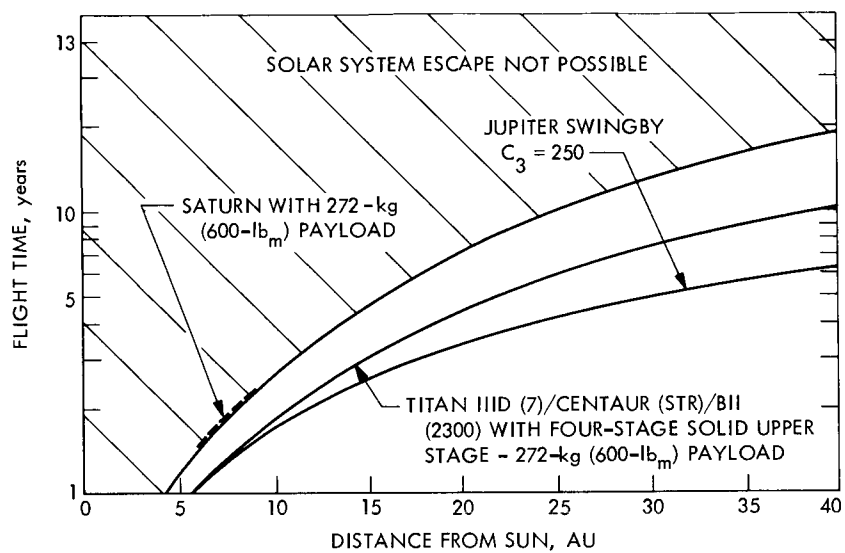
Fig. 1. Concept description

Fig. 2. Mission flight time vs. distance from the sun

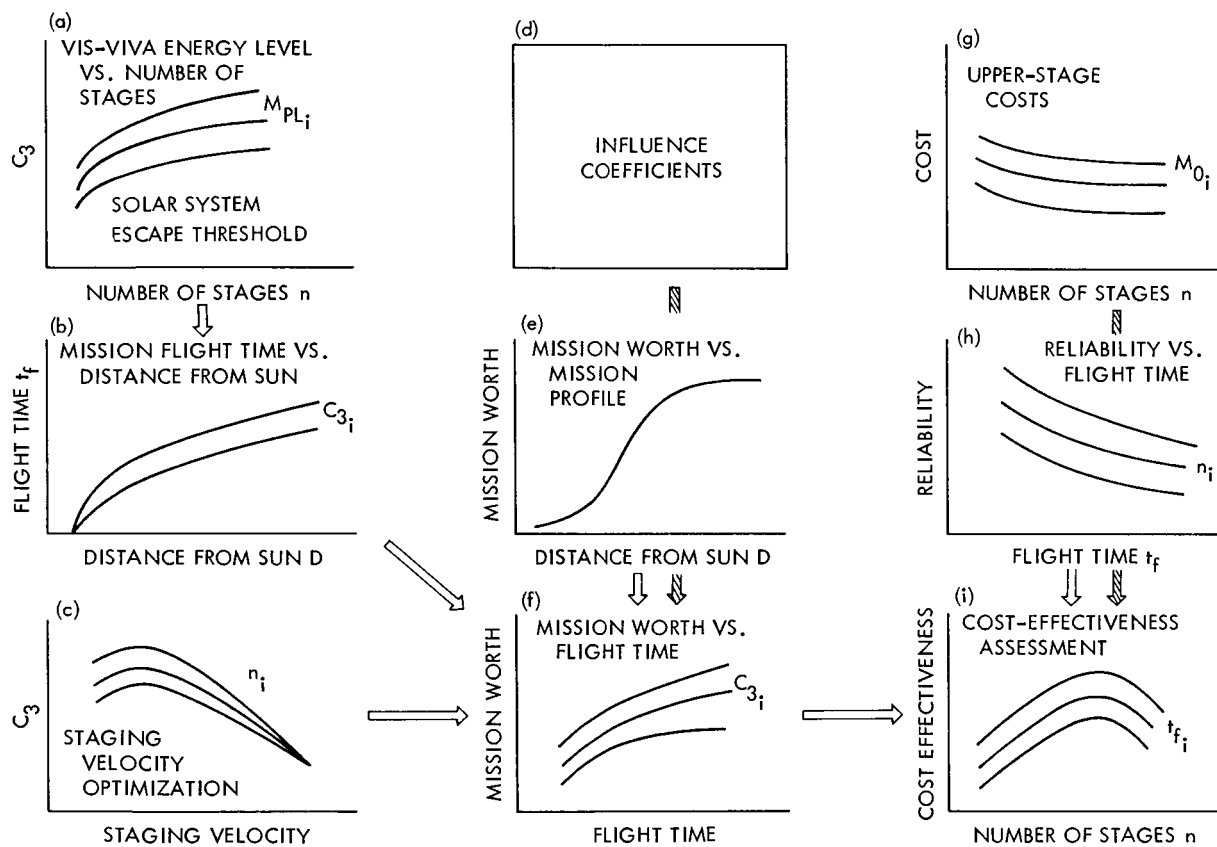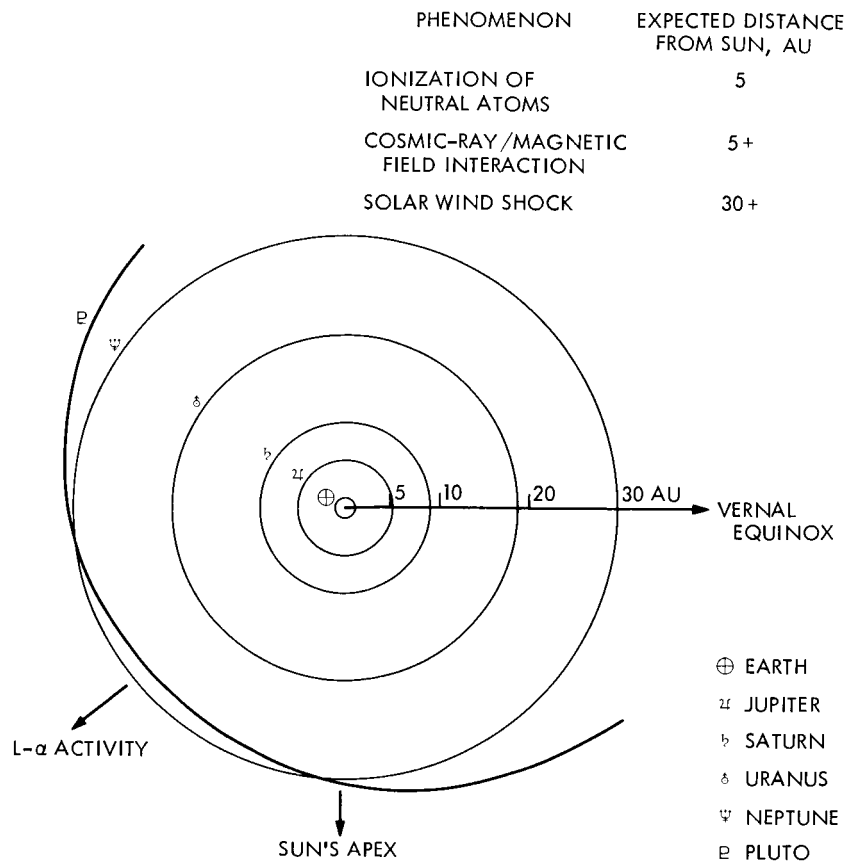Fig. 3. Cost-effectiveness tradeoff methodology

PHENOMENON	EXPECTED DISTANCE FROM SUN, AU
IONIZATION OF NEUTRAL ATOMS	5
COSMIC–RAY/MAGNETIC FIELD INTERACTION	5+
SOLAR WIND SHOCK	30+

Fig. 4. Regions of scientific interest
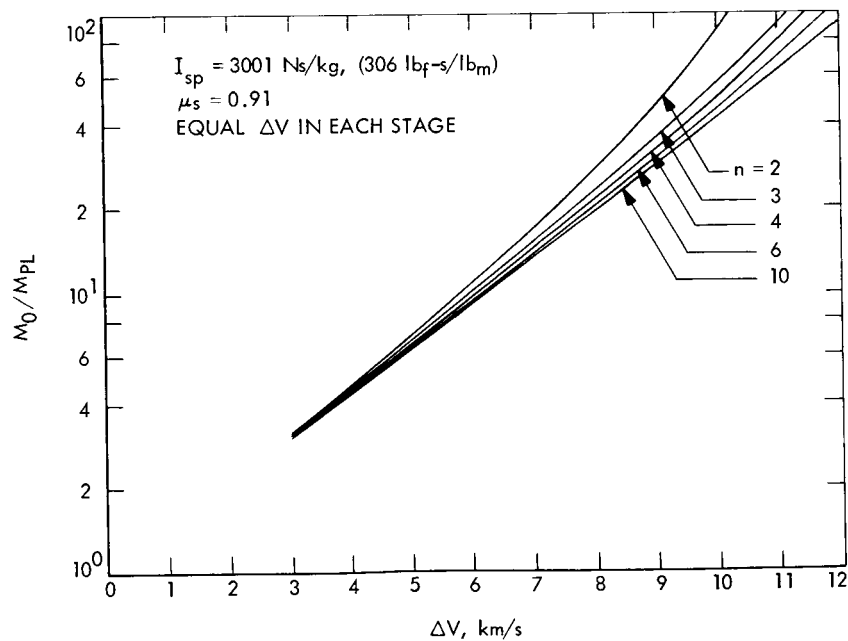
Fig. 5. M_0/M_{PL} vs. total velocity increment
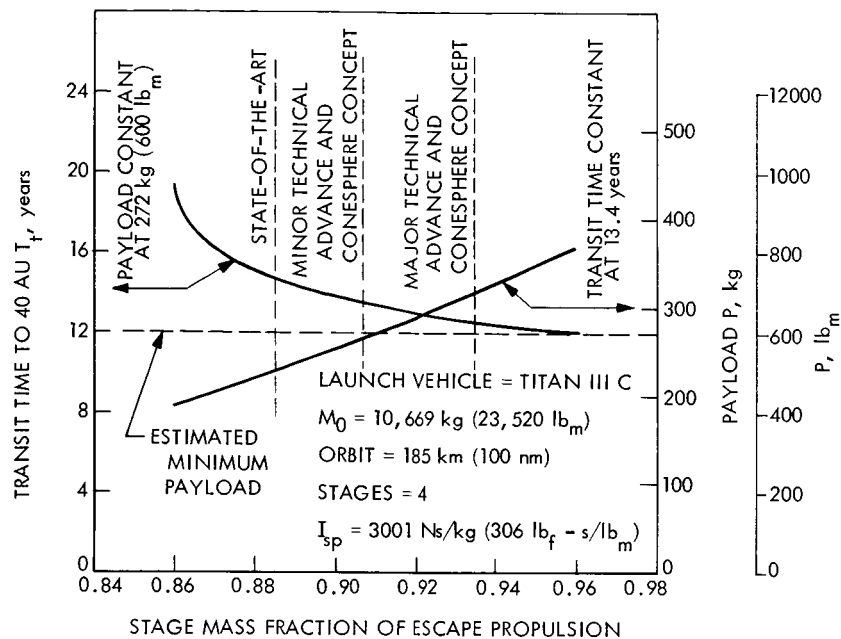
Fig. 6. Significance of stage mass fraction (Titan IIIC)
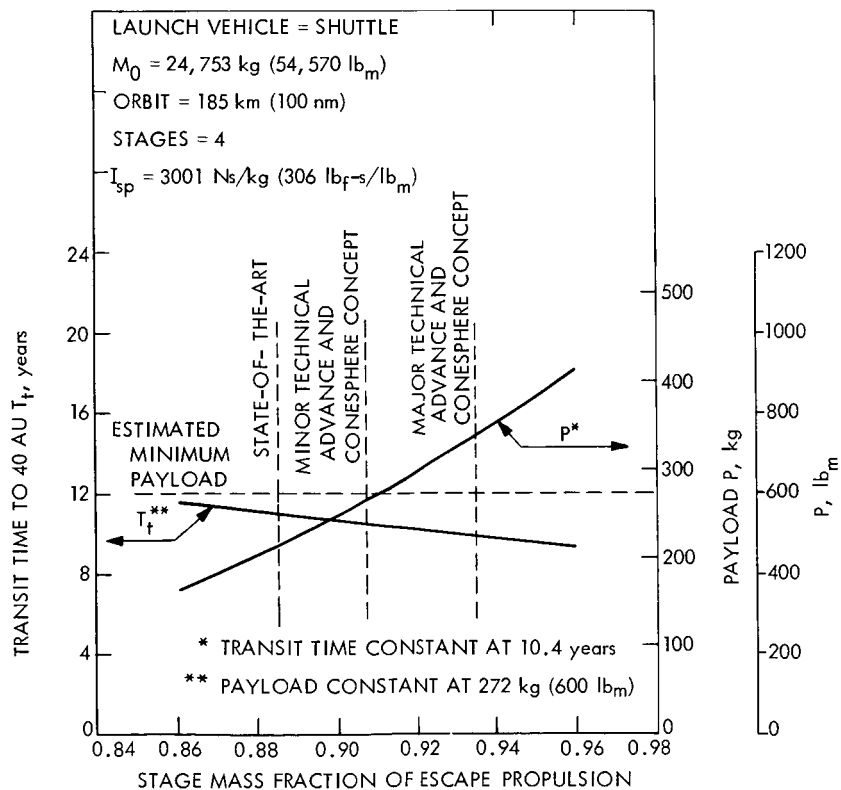
Chart (upper):
- Y-axis (left): TRANSIT TIME TO 40 AU T_f, years — 0, 4, 8, 12, 16, 20, 24
- Y-axis (right, inner): PAYLOAD P, kg — 0, 100, 200, 300, 400, 500
- Y-axis (right, outer): P, lb_m — 0, 200, 400, 600, 800, 1000, 12000
- X-axis: STAGE MASS FRACTION OF ESCAPE PROPULSION — 0.84, 0.86, 0.88, 0.90, 0.92, 0.94, 0.96, 0.98

Labels:
- PAYLOAD CONSTANT AT 272 kg (600 lb_m)
- STATE-OF-THE-ART
- MINOR TECHNICAL ADVANCE AND CONESPHERE CONCEPT
- MAJOR TECHNICAL ADVANCE AND CONESPHERE CONCEPT
- TRANSIT TIME CONSTANT AT 13.4 years
- ESTIMATED MINIMUM PAYLOAD

- LAUNCH VEHICLE = TITAN III C
- M_0 = 10,669 kg (23,520 lb_m)
- ORBIT = 185 km (100 nm)
- STAGES = 4
- I_{sp} = 3001 Ns/kg (306 lb_f - s/lb_m)

Fig. 7. Significance of stage mass fraction (shuttle)

Chart (lower):
- LAUNCH VEHICLE = SHUTTLE
- M_0 = 24,753 kg (54,570 lb_m)
- ORBIT = 185 km (100 nm)
- STAGES = 4
- I_{sp} = 3001 Ns/kg (306 lb_f-s/lb_m)

- Y-axis (left): TRANSIT TIME TO 40 AU T_f, years — 0, 4, 8, 12, 16, 20, 24
- Y-axis (right, inner): PAYLOAD P, kg — 0, 100, 200, 300, 400, 500
- Y-axis (right, outer): P, lb_m — 0, 200, 400, 600, 800, 1000, 1200
- X-axis: STAGE MASS FRACTION OF ESCAPE PROPULSION — 0.84, 0.86, 0.88, 0.90, 0.92, 0.94, 0.96, 0.98

Labels:
- ESTIMATED MINIMUM PAYLOAD
- STATE-OF- THE-ART
- MINOR TECHNICAL ADVANCE AND CONESPHERE CONCEPT
- MAJOR TECHNICAL ADVANCE AND CONESPHERE CONCEPT
- P*
- T_f^{**}
- * TRANSIT TIME CONSTANT AT 10.4 years
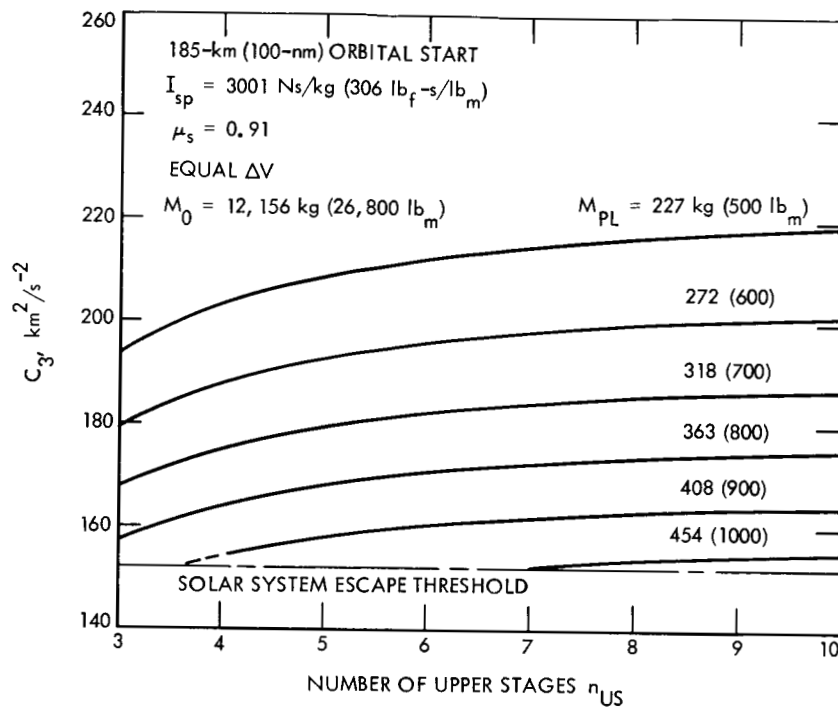- ** PAYLOAD CONSTANT AT 272 kg (600 lb_m)

Fig. 8. C_3 vs. N_{US} for solar escape--TIIID (7)/ Centaur/VUS launch vehicle
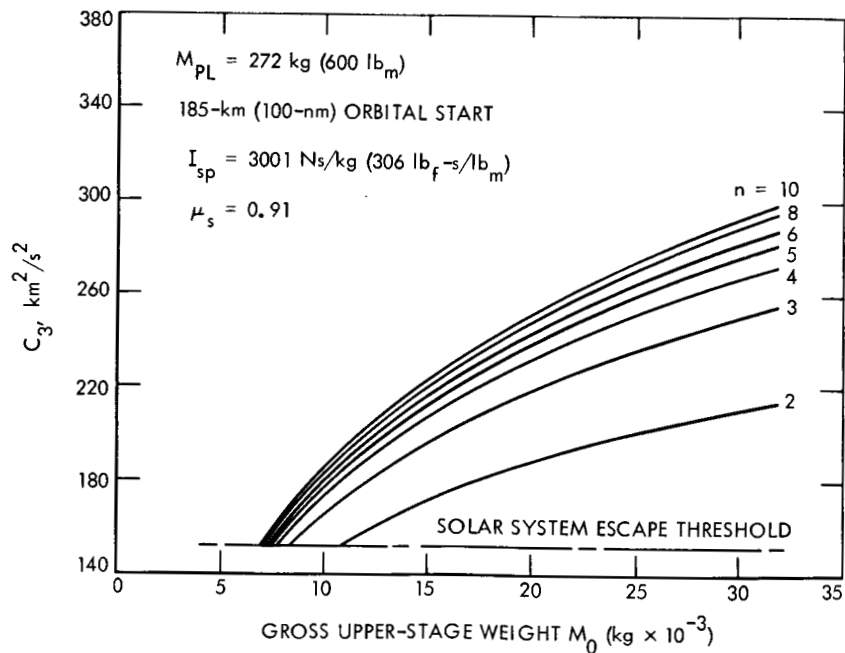

Fig. 9. Space shuttle propulsion performance capability
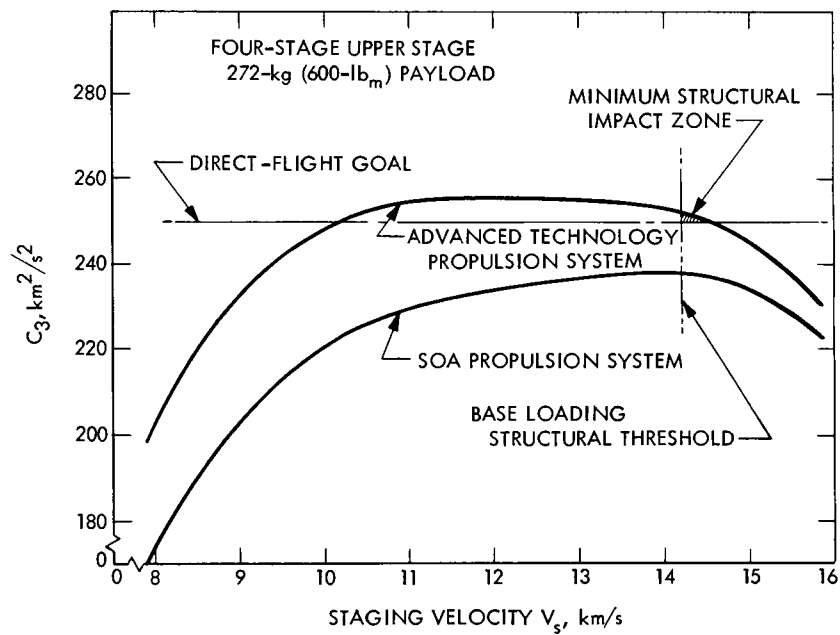
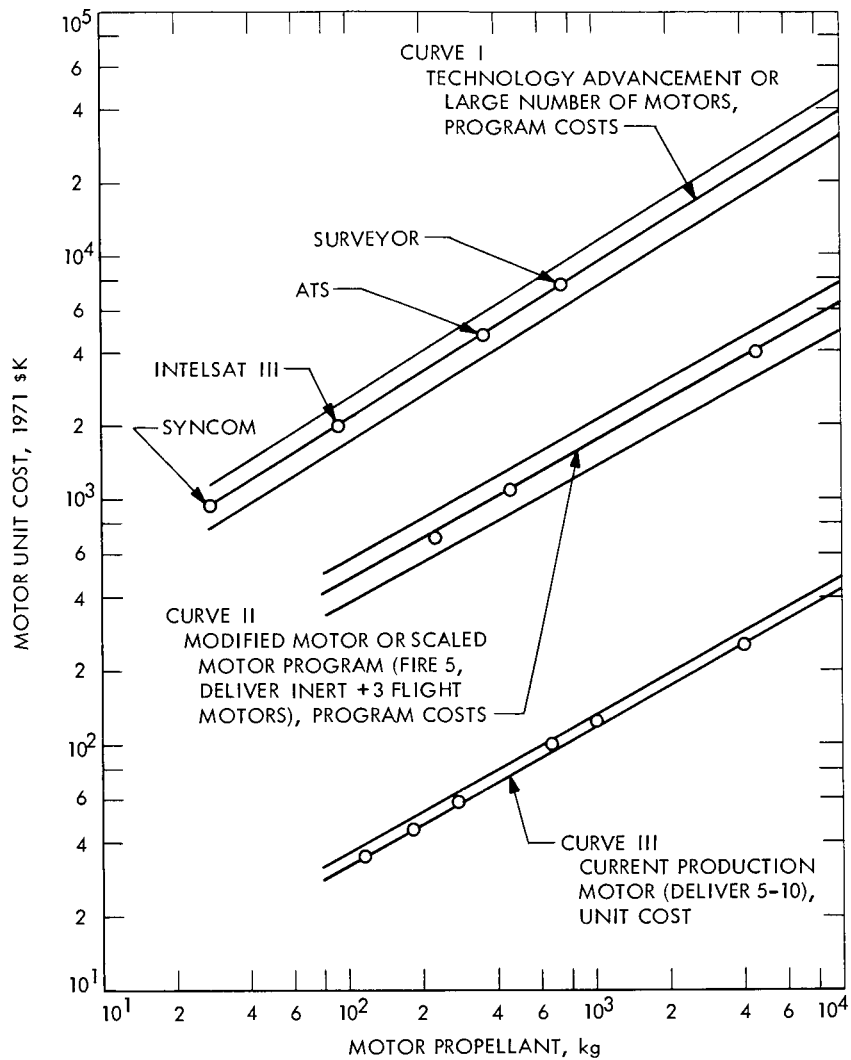Fig. 10. C_3 vs. V_S for TIIID (7)/Centaur (STR)/ BII (2300) vehicle assembly
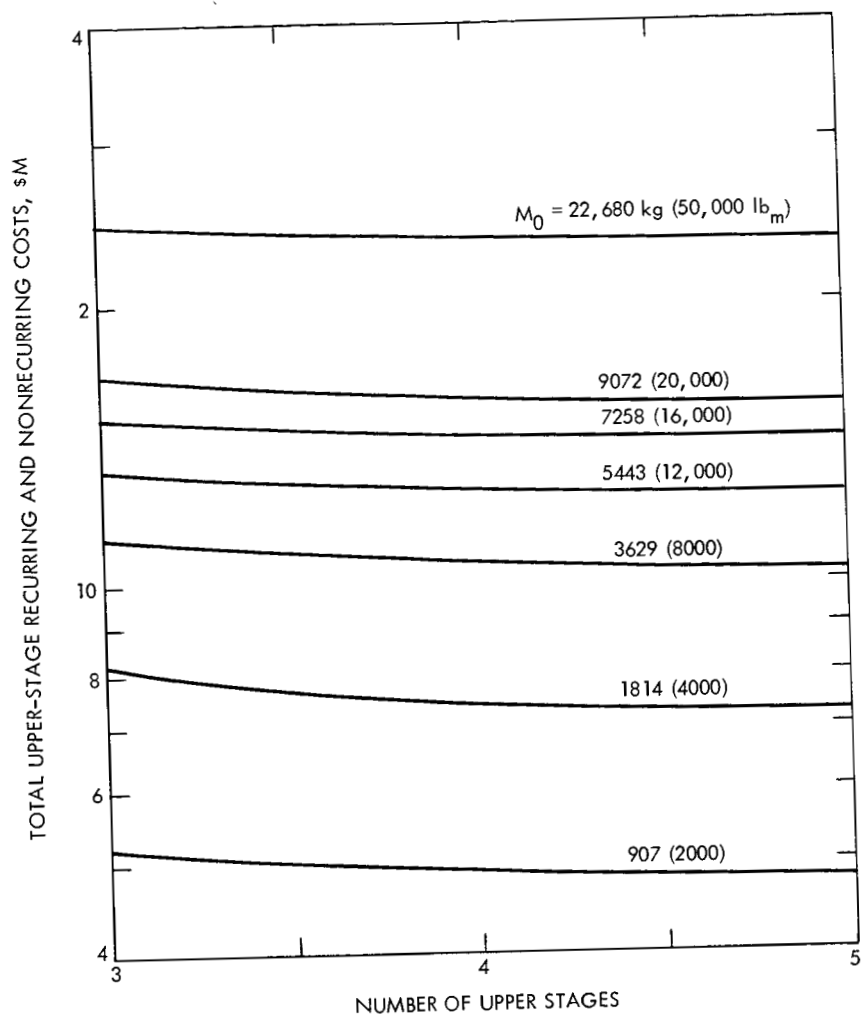
Fig. 11. Solid propellant motor costs

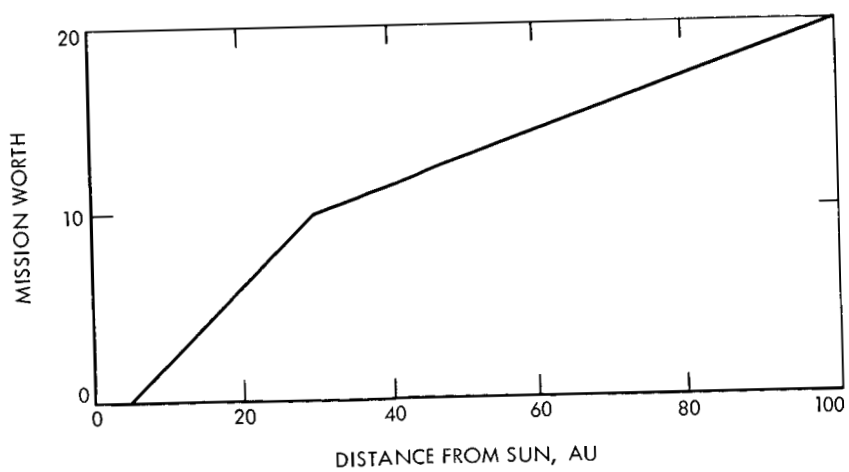Fig. 12.   Upper-stage costs vs. number of upper stages

Fig. 13.   Preliminary estimate of mission worth as
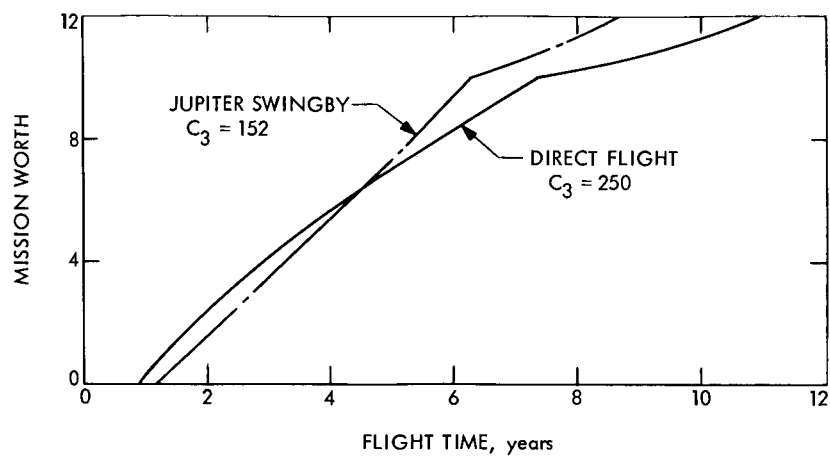a function of distance from the sun

Fig. 14. Mission worth vs. flight time--selected direct and Jupiter swingby probes
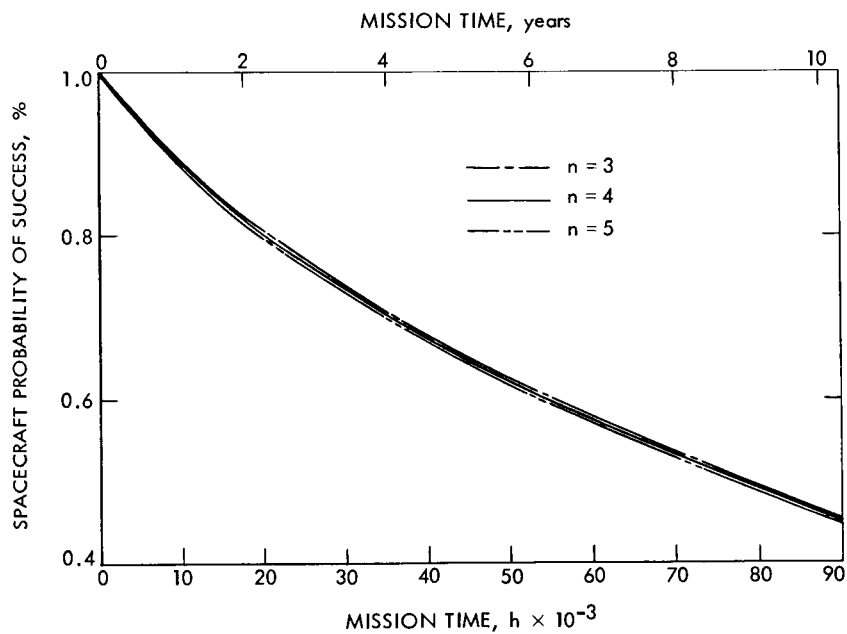

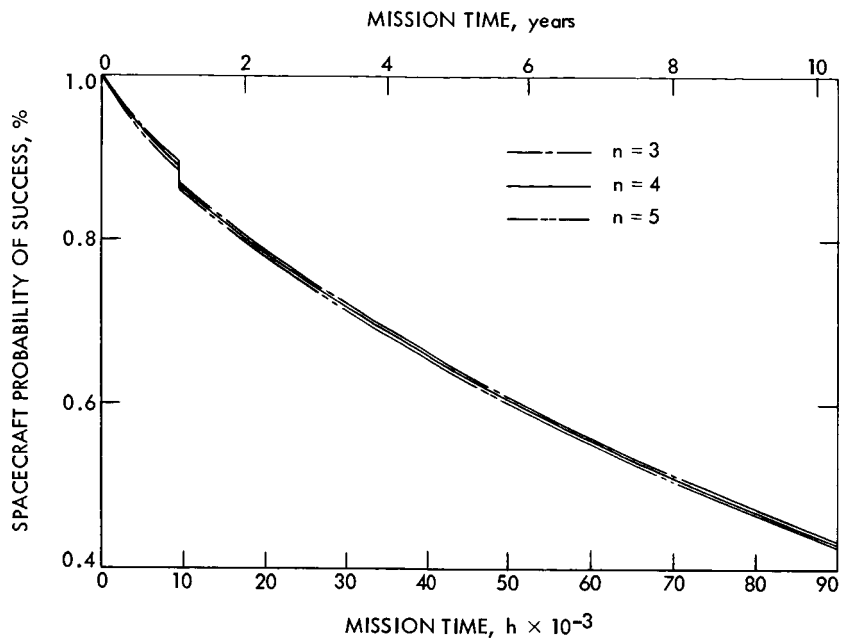Fig. 15. Spacecraft probability of success for direct flight missions

Fig. 16. Spacecraft probability of success for
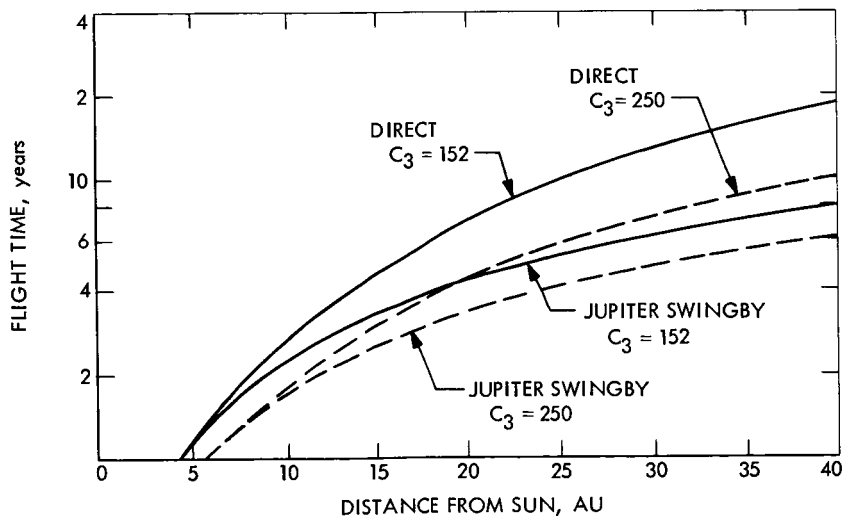Jupiter swingby missions

Fig. 17. Effect of C_3 upon mission flight time and
distance

APPENDIX A

PROPULSION TECHNOLOGY

Initial studies were oriented toward assessing the performance of today's state-of-the-art motors using aluminized propellants and estimations of the technology that could be available after about 7 years of R and D. Values derived for motor performance were:

State-of-the-Art Motors

Motor size, kg	90.72	453.6	4536
Motor size, lb_m	200	1000	10,000
Vacuum I_{sp} (ϵ = 80), Ns/kg	2844	2903	2912
Vacuum I_{sp} (ϵ = 80), lb_f-s/lb_m	290	296	297
Motor mass fraction	0.91	0.93	0.935

Predicted Performance After 7 Years R and D

Motor size, kg	90.72	453.6	4536
Motor size lb_m	200	1000	10,000
Vacuum I_{sp} (ϵ = 80), Ns/kg	2942	3001	3010
Vacuum I_{sp} (ϵ = 80), lb_f-s/lb_m	300	306	307
Motor mass fraction	0.94	0.955	0.960

State-of-the-art motors in the present context means motors that could be produced with today's knowledge and capability; the values tabulated above are somewhat higher than those observed in "motors flying today." For example, the 304-kg (664-lb_m) fourth-stage FW-4 motor for Scout (Ref. 13) has a mass fraction of 0.911 and vacuum I_{sp}, at an expansion ratio of 50, of 2805 Ns/kg (286 lb_f-s/lb_m); the corresponding state-of-the-art motor would have a mass fraction of 0.928 and a vacuum I_{sp} of 2814 Ns/kg (287 lb_f-s/lb_m).

Concurrent with the state-of-the-art motor assessment, design studies were made to reduce the interstage weight of the multi-stage propulsion system. A new, very promising concept, the "nested conesphere," was the result (Ref. 14). It is that concept and its implications which will be discussed here.

I.   NESTED CONESPHERE CONCEPT

In a conventional design of a spacecraft with a four-stage solid propulsion system, shown schematically at the top of Fig. A-1, the motors would have short length-to-diameter ratios, rather large nozzles for space operation, and would be coupled with interstage structure. In order to reduce the inert weight of the propulsion system significantly, it was proposed that the interstage structure be eliminated by using the nozzles as structure, as shown in the second configuration.

An examination of the second assembly shows that the volume efficiency is much lower than desired; the chambers would contain propellant but the relatively large nozzles would not. Therefore, in the third configuration, the chambers were reshaped and nested in the nozzle ahead in order to shorten the overall assembly length about 20%.

However, the nozzle and chamber then constitute redundant structures. Thus, in the final configuration, the three redundant nozzles would be eliminated. The chamber would be used as a propellant container during the firing of a given stage, and as a nozzle during the firing of the next stage. The integral chamber-nozzle component is then called a chamzle (see Fig. A-2).

In order for the motors to function as described, it is necessary to have a closure or isolation plug in the forward end of each chamzle -- to prevent preignition of the next motor -- and a separation mechanism (see insert Fig. A-2) to stage off the spherical portion and its nozzle after the propellant burns out of the chamzle. Staging off the aft portion by a separation mechanism, such as a flexible, linear-shaped charge, automatically produces the nozzle for the next motor firing.

In summary, the motors could operate as follows:

1.   The igniter fires the largest motor, and its propellant burns out completely. After about 5 to 10 s, a circuit in the payload section fires the flexible, linear-shaped charge of the motor, staging off the spherical section of the chamzle and its nozzle, thus creating the new nozzle for the next stage.

2. On signal from the firing circuit, the next-largest motor is ignited, expelling its nozzle isolation plug. The propellant burns out entirely, and staging is again effected, creating a new nozzle. The sequence of events is repeated for motors 3 and 4. However, all of motor 4 would probably be staged off in order to reduce the thermal-control requirement on the spacecraft.*

It should be noted that if the chamzle is to serve as a nozzle later, it probably should be made of an all-carbon composite (a carbon matrix with reinforcing carbon fibers). Such a design draws on and extends the recent all-carbon technology developed for nozzles in JPL's long-burning motor program (Ref. 15). The nozzle and aft end of the chamzle, of course, will operate while radiating heat to space, with surface equilibrium temperatures as high as 1093 to 1649°C (2000 to 3000°F).

There are assembly joints, shown as threaded members in Fig. A-2, in each motor for manufacturing and shipping purposes. Thus, there would be four chamzles with loaded propellant and one separate nozzle for the largest motor during shipment for propulsion system assembly at the Cape.

The igniters in each motor will probably be located near the motor assembly joint. The exact method and routing of firing lines to the igniters has not been fixed, though they may well come from the payload internally along the axis of the motors to the respective igniters. Laser techniques using fiber optics are under review (Ref. 16). Alternately, automatic ignition from stage to stage, with a pyrotechnic time delay between motors, is also under consideration.

At this stage in the study, the motors have been kept as simple in operation as possible. There would be no thrust termination; all motors burn to depletion. In addition, it has been assumed that there would be no thrust vector control. Thrust misalignment would be compensated for by spinning

---

*Subsequent studies may show that the chamzle shape of stage 4 should be more conventional in order to realize additional performance, even though the scaling principle for that stage would be abandoned and development costs would increase.

during motor burn. If later analysis* reveals that Jupiter swingby missions are desirable and thrust vectoring methods are needed, the design study should be extended to include that feature.

Burning times range from 80 s for the smallest motor to about 201 s for the largest. Maximum acceleration with a 272-kg (600-lb$_m$) payload would be about 6.1 g. However, for acceleration-sensitive payloads, the maximum acceleration could be reduced to about half to two-thirds that value with only a small penalty in propulsion performance.

For a 10,660-kg (23,500-lb$_m$) assembly (spacecraft and escape propulsion), the overall length would be approximately 9 m (29.7 ft) and the maximum chamzle diameter about 1.8 m (6 ft).

It should be pointed out that each motor is a true scale model of the other three. Diameters, lengths, and thicknesses are scaled by the same linear factor. As will be noted later, this is important for reducing the propulsion development costs.

II. CRITICAL DESIGN AREAS AND POTENTIAL PERFORMANCE

There are some potential problem areas in the concept; however, it is planned to initiate advanced development work on critical questions under NASA sponsorship very soon.

First, a vacuum specific impulse of 3001 Ns/kg (306 lb$_f$-s/lb$_m$) has been assumed for the new class of aluminized** hydroxy-terminated polybutadiene propellant currently under development. The best predicted value for today's propellant is 2903 Ns/kg (296 lb$_f$-s/lb$_m$), 98 Ns/kg lower than the assumed value However, a new concept under examination (Ref. 17) for raising the efficiency of metal combustion processes in solid propellants (ammonium perchlorate with occluded aluminum) may provide the potential improvement indicated. If, alternately, no increase in I$_{sp}$ were realized, an equivalent

---

*Some preliminary calculations indicate that a Jupiter swingby could be carried out by despinning the spacecraft after staging off the four solid propellant motors and providing midcourse correction, impulse control, and three-axis attitude stabilization with electric thrusters and micropulsers. Thrust vectoring the solid motors probably can be avoided.

**Berylliumized solid propellants were omitted from the study at this time because of the complicating factor of toxicity.

reduction in mass fraction of 0.007 from the mass fractions noted later would result. Although that is a significant penalty, it is not enough to jeopardize the proposed propulsion concept.

The second problem area, preignition of propellant from high heat transfer in the chamzle, arises because the latter is made of carbon, and carbon is a good thermal conductor. Shortly after ignition, heat will be conducted from the nozzle along the spherical wall. Although chamzle insulation has been provided to isolate the propellant and prevent preignition, a good thermal analysis must be made to be sure that preignition of the propellant and the explosive separation device won't occur.

The third problem area, pyrotechnic separation of the carbon chamzle, or staging, is critical to the concept. The carbon chamzle is brittle, even though the carbon reinforcement fibers toughen the structure markedly. When staging is attempted, firing the flexible, linear-shaped charge might crack, or even shatter, the next-stage nozzle. Early experimental tests are scheduled to check the validity of the separation concept.

A backup design is currently under examination, but it is too early to assess its merits and demerits. It would use detonation principles to shape the shock of the chamzle and fracture mechanics to control the cleavage and fracture environment. The penalty in mass fraction, if the backup must be used, is not expected to be large.

The fourth problem area involves the advancement required in the technology of the all-carbon composites used as nozzles and chamzles. The present all-carbon technology employs a fabrication technique based on a rosette layup. Recently, two JPL nozzles fabricated in this way were statically fired successfully in three out of three tests without structural failures and with negligible erosion. Thiokol Chemical Corporation has also satisfactorily fired two out of two all-carbon nozzles. If this technology were extended from the nozzle to include the chamber, and those concerned believe it can be, the conesphere motor mass fraction estimate would be 0.917 and the overall stage mass fraction 0.907.

However, the technology offers a potential capability well beyond that (Ref. 18). The new method of fabrication would utilize filament-winding of high strength, high-modulus carbon filaments (such as Thornel 50), and

formation of the carbon matrix in the interstices between fibers by chemical vapor deposition (CVD). Filament-wound cylindrical and other test specimens have shown tensile and interlaminar shear values 2 to 2-1/2 times those of the rosette layup material (Refs. 19 and 20). If those mechanical properties can be realized in the chamzle, the average motor mass fraction should increase to about 0.945 and the stage mass fraction to about 0.935. For comparison, today's state-of-the-art motors have a motor mass fraction of 0.93 and a stage mass fraction, including interstage structural weights, of 0.885. Figures 6 and 7 in the text show the significant increase in propulsion payload that results from such an increase in stage mass fraction and use of the conesphere concept.

It is self-evident that a major development effort in the carbon-composite technology area will be necessary if the advanced concept is to be realized. Fortunately, other investigators, the Naval Ordnance Laboratory and the Sandia Corporation, are also developing carbon composites, and their work would supplement the planned technology efforts.

III. PROPULSION DEVELOPMENT COSTS AND RECURRING COSTS

Any concept that requires four completely new motors based on very advanced technology would result in large development costs if the conventional method of developing and procuring motors were adopted. Winston Gin (Ref. 21) has determined the relationship of program development costs to motor size for such solid propellant motors as SYNCOM, Intelsat III, the Applications Technology Satellite apogee motor, and Surveyor, i.e., programs in which the state-of-the-art was being advanced, as it is in the motors under consideration (see Fig. 11, curve I). With that relationship as a basis, the development costs for four stages of escape propulsion totaling 10,660 kg (23,500 lb$_m$) have been estimated at 61.1×10^6, assuming a conventional development approach. See Table A-1 for the breakdown by stages.

For the concept under discussion, an alternate approach is advocated. It would capitalize on the scaling laws in order to reduce propulsion development costs significantly and is based upon the following rationale. It has been demonstrated in the Sergeant program, and verified in the SYNCOM and Applications Technology Satellite motor programs, that subscale motors of a much larger motor could be used to predict the pressure and thrust time histogram of the larger motor (Ref. 1) if all motor dimensions are scaled

linearly and the charge design and propellant are maintained. A stress analysis of the motor and the propellant charge also reveals that, provided body forces are relatively insignificant, stresses in the motor and propellant are independent of scale. The heat transfer in the nozzle scales as $D^{0.2}$ and results, therefore, in slightly conservative conditions on scaling up. The specific impulse of the aluminized propellant tends to increase slightly with increasing size because two-phase flow losses are lower at the larger size.

Combustion instability and charge creep (or slump) do not scale; however, the latter appears to be no problem with the propellants and motor sizes proposed. In the past, combustion instability was observed only infrequently after aluminum was introduced into solid propellant formulations, but as propellants have become more energetic, it has reappeared on some occasions (as may be the case with the powered spacecraft application). Fortunately, as Brownlee (Ref. 22) showed, the tendency for a motor to resonate acoustically decreases with decreasing chamber pressure and with decreasing L/D. (The tailored solid upper stages will have low values in both cases.) The tendency is reduced even further if one changes from Brownlee's internal radial burning design to an end-burning design. If instability were encountered, there are several methods for its elimination, such as resonance rods or baffles, though none is ideal or without some performance penalty.

In summary, this scaled-motor approach consists of developing one of the smaller motors in order to advance the technology and the high level desired at the lowest cost, while using numerous small motors to evaluate all problematical aspects in order to establish a high confidence in the reliability of the basic design. Because the larger motors for all other stages are scaled-up motors, ballistically and stresswise, very little additional development would be needed. The larger motors would be fabricated directly, then three motors each would be delivered. Successful static firings for any one motor would constitute successful static firings for all motor sizes because each is a scale model of the others. This technique permits use of a single optimum-sized motor in each stage, so that near-optimum spacecraft performance would be available at high reliability and high confidence levels.

The cost of developing the first, smallest motor through flight, because of the comprehensive program, is estimated at $9.5 million, almost double

the 5.2 million estimated for the same motor using conventional development methods (see Table A-1). With the smallest motor qualified, the three larger, linearly scaled motors would be manufactured, and their performance would be verified in a five-motor qualification program (see curve II of Fig. 11). Motor manufacturers are currently performing five-motor qualification testing of modified motors. These are off-the-shelf motors that are lengthened, modified with a different propellant, or altered slightly in design. Using industry's costs for modified motor programs for the three largest motors, the total proposed scaled-motor program would be $19.1 million, or about 30% of the more conventional development program costs. Both program totals include propulsion costs for development to flight, qualification firings, and delivery of one inert motor and three flight motors for each of the four stages.

Drawing on industry's experience, from fixed-price production contracts, the production or recurring cost of one set of four motors, when ordered in lots of five or ten, would be about $0.8 million to 1 million per set of four. Obviously, these cost estimates must be verified when the system design has been looked at in greater detail.

IV. CONCLUSIONS

As a result of the propulsion analyses to date, it can be concluded that

1. A stage mass fraction of 0.935 is technically feasible through use of the conesphere concept and the advanced all-carbon composite technology; growth potential beyond this appears to exist.

2. The cost of developing four scaled motors can be reduced to about 30% of conventional development costs through application of the scaling laws.

Table A-1. Cost estimates in 1971 dollars -- spacecraft
escape propulsion

Stage motor weight		Conventional development, $\$ \times 10^{-6}$	Proposed scaled-motor programs, $\$ \times 10^{-6}$	Production cost, $\$ \times 10^{-6}$
kg	lb_m			
410	904	5.2	9.5	0.08
1,034	2,278	9.3	1.7	0.13
2,610	5,754	16.6	2.9	0.22
6,606	14,564	30.0	5.0	0.38
Totals 10,660	23,500	61.1	19.1	0.81

CONVENTIONAL DESIGN

ELIMINATE INTERSTAGE STRUCTURE
BY USING NOZZLES

SHORTEN AND UTILIZE VOLUME
BETTER BY RESHAPING CHAMBER

ELIMINATE REDUNDANT STRUCTURE BY
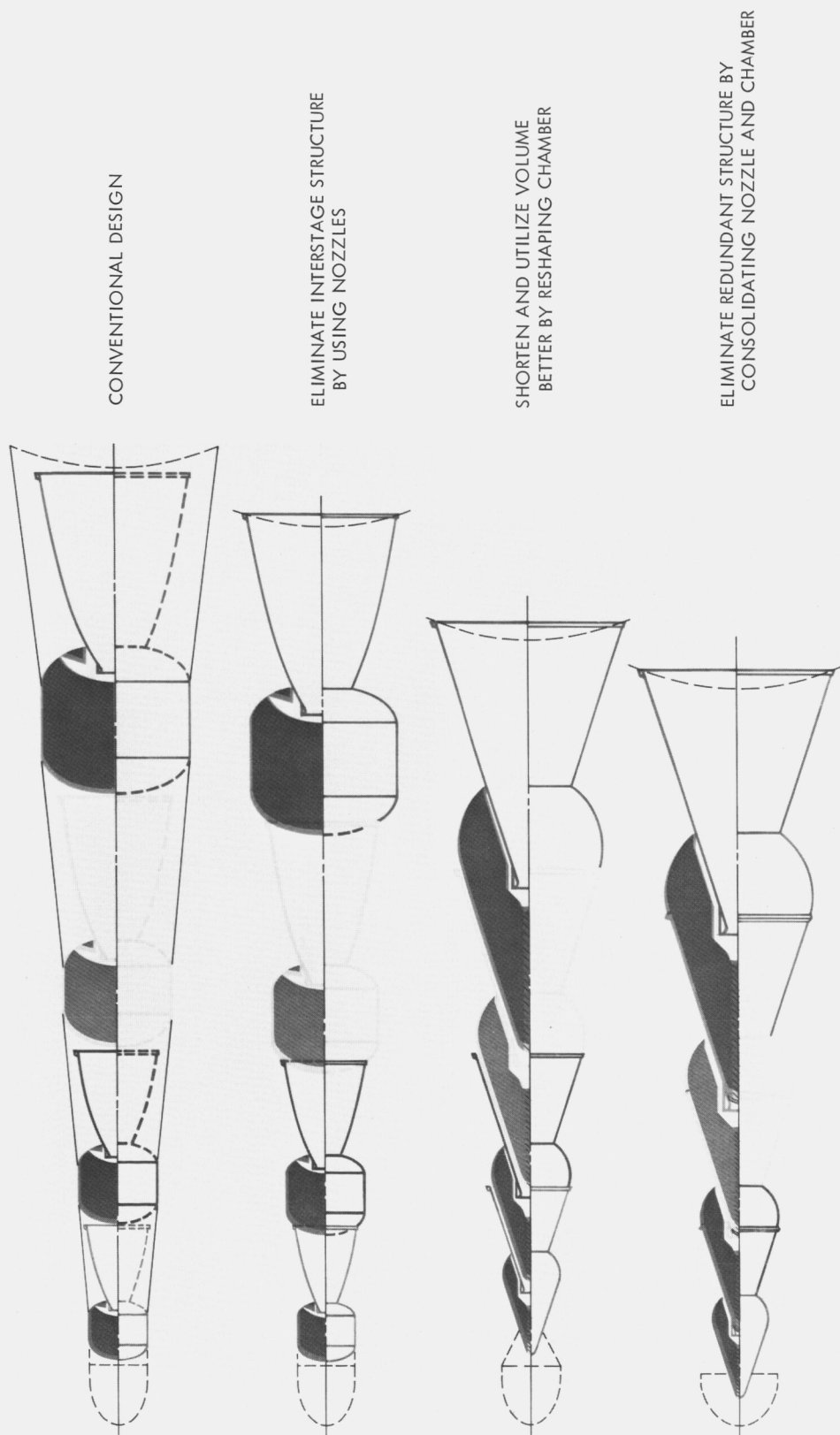CONSOLIDATING NOZZLE AND CHAMBER

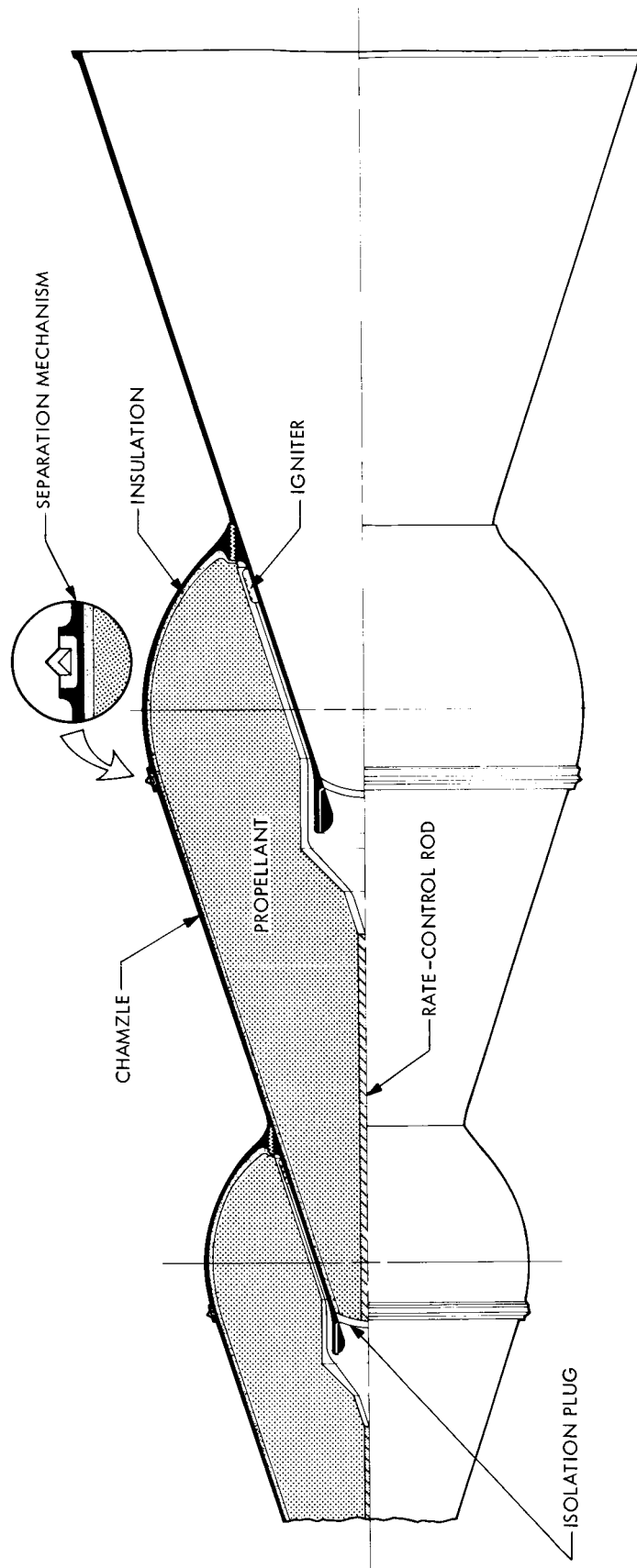Fig. A-1. Evolution of conesphere concept

Fig. A-2. Conesphere motor

APPENDIX B

SAMPLE COST-EFFECTIVENESS CALCULATION

Determine the cost-effectiveness rating for a Jupiter swingby alternate utilizing a Titan IIID basement vehicle.

Assumptions

1. The mission consists of two flights in the 1980 time era.

2. Upper-stage costs include the cost of development and delivery of two flight hardware subsets plus one spare.

3. Spacecraft costs include the development and delivery of two flight units plus one prototype that could be modified into flight configuration as required.

4. All costs are in 1971 dollars.

Costs

1. Basement Vehicle [TIIID (2 × 1205/Core I/Core II)] (Ref. 5)

   Recurring costs

   Hardware (production rate: 4/year)

Common core--Martin Marietta	$1.76M
Liquid engines--Aerojet	2.26
Solid rocket motors--UTC	5.70
GFE	0.08
GSE/TD	0.32
Acceptance propellants	0.09
Changes/growth	0.49
Hardware, peculiar	1.20

   Other hardware

Shroud	0.20
Guidance	0.15
Adaptor/spin table	0.04
Total hardware	$12.29M

Support (launch rate: 4/year)

Launch services core I/II	$1.78M
Engines - stages I and II	0.25
SRMs	0.56
Transportation	0.05
Propellants	0.15

Other support

ITL D&M	0.75
AF travel	0.08
Range costs	1.20

Total support	$4.82M
Total vehicle	$17.11M
Mission hardware ($17.11M × 2)	$34.22M

Nonrecurring costs
(Mission-peculiar engineering
and hardware costs for first
flight only) $1.2M

Total basement vehicle costs (2 flights)	$35.42M

2. Spacecraft escape propulsion system

Development costs	$4.40M
Flight hardware (four-stage)	$5.53M
Total escape propulsion	$9.93M

3.	Spacecraft costs	$75.0M
4.	Mission operations	$40.0M
5.	Management and contingencies	$35.0M

Overall program costs $195.35M

Reliability

    Probability of mission success   0.505

Mission worth (at 40 AU)   11.5

Cost-effectiveness assessment

$$CE = \frac{PW}{C_T} = \frac{0.505\ (11.5)}{195.35}$$

$$= 0.029729\ (\text{probability of success} \times \text{mission worth}/\$M)$$

REFERENCES

1. Landsbaum, E. M., and Schumacher, J. C., "Comparison of Ballistic Properties of Scale-Model and Full Size Sergeant Motors," Publication No. 141, Jet Propulsion Laboratory, Pasadena, Calif., 1958. (CONFIDENTIAL)

2. Shafer, J. I., "Propulsion Cost Estimates," Internal Document, IOM 381-71-75, Jet Propulsion Laboratory, Pasadena, Calif., October 6, 1971.

3. Launch Vehicle Estimating Factors, NASA Document NHB 7100.5, January 1971.

4. Phen, R. L., "Preliminary Study of the Impact of the Space Shuttle on Planetary Propulsion," Internal Document, Jet Propulsion Laboratory, Pasadena, Calif., February 25, 1971

5. Economic Data Document, 1971, OSSA Document BMI-NLVP-DD-3-(71), 1971.

6. "TOPS Spacecraft Probability of Success for One Spacecraft," TOPS Project Review III, Internal Document, Jet Propulsion Laboratory, Pasadena, Calif., April 9-10, 1970.

7. Robillard, C. L., Summary of the Meeting of the Panel on Reliability of Large Solid-Propellant Motors, Technical Memorandum 33-219, Jet Propulsion Laboratory, Pasadena, Calif., May 10, 1965.

8. Martin, P. J., Reliability Estimation for Chemical Propulsion System, SRI Project MSU-8075, Stanford Research Institute, Stanford, Calif., May 1970.

9. Don, J. P., and Phen, R. L., Application of Hybrid Propulsion Systems to Planetary Missions, Technical Memorandum 33-483, Jet Propulsion Laboratory, Pasadena, Calif., November 1, 1971.

10. Feasibility Study for a Multi-Mission Electric Propulsion Spacecraft (Pioneer Concept), TRW Report No. 18305-6001-R000, Redondo Beach, Calif., June 18, 1971.

11. Solar Electric Multi Mission Spacecraft (SEMMS) Phase A Final Report, Technical Summary, Internal Report No. 617-2, Jet Propulsion Laboratory, Pasadena, Calif., September 1971.

12. Study of a Common Solar-Electric-Propulsion Upper Stage for High-Energy Unmanned Missions, Vol. I, TRW Report No. 16552-6006-R0-00, Redondo Beach, Calif., July 1971.

13. Rocket Motor Manual, SPIA/MI Vol. II, Unit 480, Chemical Propellant Information Agency, Johns Hopkins University, Applied Physics Laboratory, Silver Spring, Maryland, October 1968. (CONFIDENTIAL)

14. Bamford, R. and Shafer, J. I., "Staged Solid Propellant Motors," NASA Invention Report 30-13080, October 8, 1971.

15. Bailey, R. L. and Carmichael, D. E., Pyrolyzed Materials Nozzle, 1971 JANNAF Combined Propulsion Meeting, CPIA Publication 219, Vol. I, pp. 153-167, Chemical Propellant Information Agency, Johns Hopkins University, Applied Physics Laboratory, Silver Spring, Maryland, October 1971.

16. Menichelli, V. J., and Yang, L. C., Sensitivity of Explosives to Laser Energy, Technical Report 32-1474, Jet Propulsion Laboratory, Pasadena, Calif., April 30, 1970.

17. Simmons, G. M., and Shafer, J. I., "Solid Propellants Using Occluded Metal Fuel," NASA Invention Report 30-11975, December 6, 1971.

18. Coulbert, C. D., Pyrolytic Refractory Materials for Spacecraft Thrust Chambers, Composite Thrust Chambers for the Period July 23, 1968 to Feb. 22, 1970, Report No. S989, The Marquardt Co., Van Nuys, Calif., May 7, 1971.

19. Kotlensky, W. V., and Bauer, D. W., Mechanical Properties of Isothermal CVD Carbon Infiltrated Carbon and Graphite Filament Wound Cylinders, Supertemp Co., Santa Fe Springs, Calif. Paper presented at 10th Biannual Conference on Carbon at Lehigh University, Lehigh, Pa., June 1971.

20. Private communication on interlaminar shear strength between C. Coulbert of the Jet Propulsion Laboratory and James Warren of Supertemp, Santa Fe Springs, Calif., March 1971.

21. Gin, W., Review of Selected Problems in the Utilization of Solid Propellant Rocket Motors in Space, Technical Memorandum 33-292, Jet Propulsion Laboratory, Pasadena, Calif., August 15, 1966.

22. Brownlee, W. G., Experimental Investigation of Unstable Combustion in Solid-Propellant Rocket Motors, External Publication No. 824, Jet Propulsion Laboratory, Pasadena, Calif., January 1, 1960.